

# Final report

## 1.1 Project details

<b>Project title</b>	Protection of Power Electronically Interfaced LV Distributed Generation Networks (PRO-NET)
<b>Project identification (program abbrev. and file)</b>	Energinet.dk project no.10762
<b>Name of the programme which has funded the project</b>	ForskEL
<b>Project managing company/institution (name and address)</b>	TUBITAK UZAY ODTU 06531 Ankara, Turkey
<b>Project partners</b>	Department of Energy Technology, Aalborg University SIMULA Research Laboratory
<b>CVR (central business register)</b>	29102384
<b>Date for submission</b>	Jun 21st, 2016

## 1.2 Short description of project objective and results

### English version:

The PRO-NET project is fully titled as "PROTECTION OF POWER ELECTRONICALLY INTERFACED LV DISTRIBUTED GENERATION NETWORKS". The project aims to investigate the emerging problems of and develop new solutions to the protection system of distribution networks with power-electronic-based DG integration. The main results of the project include: understanding of the impacts of DG integration on protection performance, methods to alleviate these impacts (i.e. methods from the protection perspective or DG control perspective or the perspective of coordination between protection and DG control), control strategies of DG in post-fault stage for stable islanding operation, effective and reliable communication system to support the protection and control methods.

### Danish version:

Projektet PRO-NETs fulde titel er "PROTECTION OF POWER ELECTRONICALLY INTERFACED LV DISTRIBUTED GENERATION NETWORKS". Projektet har til formål at undersøge de nye problemer der opstår og udvikle nye løsninger til beskyttelse af distributionsnet med effektelektronisk baseret DG integration. De vigtigste resultater af projektet omfatter: Undersøgelse af virkningerne af DG integration på beskyttelsens funktion, metoder at afhjælpe disse (eventuelle negative) virkninger (dvs. metoder set fra beskyttelsens perspektiv eller DG kontrollens perspektiv eller fra perspektivet af en koordinering mellem beskyttelse og DG kontrol), kontrol strategier for DG i post-fejl forløbet for overgang til stabil Ø-drift samt et effektivt og pålideligt kommunikations system til at understøtte de valgte metoder for beskyttelse og kontrol.

## 1.3 Executive summary

The PRO-NET project is fully titled as "PROTECTION OF POWER ELECTRONICALLY INTERFACED LV DISTRIBUTED GENERATION NETWORKS". The partners include the Turkish team (TUBITAK UZAY), the Norwegian team (SIMULA Research Laboratory) and the Danish team (Aalborg University). TUBITAK, Turkey is the project coordinator.

### Background:

The PRO-NET project was proposed based on the background that a large number of dispersed generation (DG) units, including renewable energy sources such as wind turbines, PV generators, fuel cells together with Combined Heat and Power (CHP) plants, are being integrated into power systems at distribution level, and power electronic converters have gained wide application in the distributed system. Although this brings the advantages of flexible onsite generation and low carbon emission, it also presents new challenges to the operation of the distribution networks.

The new characteristics of distribution networks due to integration of renewables and application of power electronics include more complicated power flow profiles, changed short circuit capacities, stochastic generation, need for communication system in protection and control, etc. As a result, the performance of the protection system of distribution networks will be deteriorated or even become non-functional if the conventional protection schemes were kept unchanged.

Therefore, the PRO-NET project aims to develop the communication technology enhanced intelligent protection and post fault control methods for distribution systems with large scale renewable energy generation units and power electronic converters. The developed protection and control methods would minimise the risks of losing power supply in an abnormal situation by stably operating of a local system in an island mode if the power system at a higher level fails, and restoring normal operation as quickly as possible.

**Working packages:**

The PRO-NET project is divided into 5 working packages (WPs) as shown in table 1.3.1.

Table 1.3.1. Working package list

WP No.	WP title	Lead participant
WP1	Project management	TUBITAK UZAY
WP2	Analysis & Protection	TUBITAK UZAY
WP3	DG modelling & Control	AAU
WP4	Communication system	SIMULA
WP5	Dissemination activities	All

More specifically, the working tasks are distributed as follows:

- Study the characteristics of distribution system with large number of renewable energy generation units and power electronic interfaced devices, (TUBITAK UZAY)
- Model the distributed generation systems (AAU)
- Develop the intelligent and adaptive protection methods (TUBITAK UZAY)
- Establish control methods to stabilising the post-fault islanding system (AAU)
- Develop cost effective and reliable communication system to support the protection and control methods (SIMULA)
- Integrated simulation platform including communication system and power system (SIMULA)
- Overall system performance evaluation (All)
  - Integrated off line Simulations
  - Real Time HIL Simulations
  - Laboratory Scale Tests

**Technical results:**

The technical results of the PRO-NET project include:

- understanding of the impacts of DG integration on protection performance;
- methods to alleviate these impacts
  - methods from the protection perspective
  - methods from DG control perspective
  - coordination between protection and DG control);
- control strategies of DG in post-fault stage for stable islanding operation;
- effective and reliable communication system to support the protection and control methods.

**Utilization:**

These technical results are expected to be beneficial for distribution system operators, consumers in LV residential areas and investors, and are expected to be utilized to realize more reliable, sustainable and economical smart distribution networks, with increased renewable integration and reduced green-house gas emission and environmental impacts. Specifically, the understanding of the impacts of DG integration on protection performance can be utilized in updating the DG connection regulations of emerging distribution systems with dominant renewable power generation (e.g. wind, solar); the mitigation methods from the protection perspective (i.e. adaptive protection) can be utilized by the protection manufacturers and distribution system operators to build a protection system more suitable for the future distribution systems; the control methods of DG during and after faults can be used by the manufacturers and owners of DGs to produce and operate the DGs in a way obeying with the regulations of the future distribution systems.

The technical results are also expected to be used as the foundation of further research activities and teaching activities related to the topics of distribution system protection, distribution generation control and communication technology in power systems.

**1.4 Project objectives**

As mentioned in 1.3, the PRO-NET project aims to develop the communication technology enhanced intelligent protection and post fault control methods for distribution systems with large scale renewable energy generation units and power electronic converters. The main objectives of the PRO-NET project are to:

- Study the characteristics of emerging distribution system with large number of renewable energy generation units and power electronic interfaced devices,
- Model the distributed generation systems
- Develop the intelligent and adaptive protection methods
- Establish control methods to stabilising the post-fault islanding system
- Determine cost effective and reliable communication system to support the protection and control methods
- Evaluate overall system performance

For the work plan, adjustments have been made due to the different time schedules of partners. The Norwegian team (SIMULA) received the funding from its agency (RCN) from 2012 as originally planned. The Turkish team (TUBITAK UZAY) started receiving the funding from its own agency from 2013, which was delayed due to their institution reorganization. To synchronize the project with TUBITAK UZAY, the Danish team (AAU) started receiving the funding from its own agency (ENERGINET.DK) also from 2013. This different time schedule challenged the synchronization of the project. However, RCN made a very good suggestion to extend the Norwegian part for one year so that the three partners were able to be synchronized in making the results and matches with the tasks schedule.

Each partner in the consortium made good contributions in its own field and the collaboration among partners is close in the project. The PI presented impressive leadership and finished the project successfully.

Three project meetings were held in the process of the PRO-NET project: a kick-off meeting in May 2013 (Istanbul, Turkey); the second project meeting in April 2014 (Aalborg, Denmark); and the final project meeting in December 2015 (Oslo, Norway). In each meeting, all the partners shared results and discussed the collaborative tasks to do. In the final meeting, the three partners discussed extensively on producing a very high-quality research paper by joining all results.

For the Danish team, the resources are efficiently used mainly for employing the research employees and travelling for project meetings and conferences..

## **1.5 Project results and dissemination of results**

### **1.5.1 Main activities and technical results**

#### **1.5.1.1 Brief description of work task distributions**

As stated in 1.3, the working tasks are distributed in the following way among the three partners in the consortium:

- Study the characteristics of distribution system with large number of renewable energy generation units and power electronic interfaced devices, (TUBITAK UZAY)
- Model the distributed generation systems (AAU)
- Develop the intelligent and adaptive protection methods (TUBITAK UZAY)
- Establish control methods to stabilising the post-fault islanding system (AAU)
- Develop cost effective and reliable communication system to support the protection and control methods (SIMULA)
- Integrated simulation platform including communication system and power system (SIMULA)
- Overall system performance evaluation (All)
  - Integrated off line Simulations
  - Real Time HIL Simulations
  - Laboratory Scale Tests

The research activities and technical results by the Danish team (AAU), namely, the distributed generation system modelling and the distributed generation control strategies during and after fault, will be described in detail in 1.5.1.2. The research activities and technical results by the Turkish team (TUBITAK UZAY) and the Norwegian team (SIMULA) will be briefly introduced in 1.5.1.3.

#### **1.5.1.2 Tasks conducted by AAU**

As assigned in the PRO-NET proposal, the Danish team (AAU) fulfilled the working tasks "modelling the distributed generation system" and "DG control strategies to stabilise the post fault islanding system". In addition, some closely relevant work has also been conducted by the AAU team to make the research more systematic, which includes a comprehensive literature review on the topic of protection of distribution systems with DG integration, short circuit analysis of distribution systems with DG integration (especially inverter-based DG), and control strategies of inverter-based DG during a fault for the purpose of maintaining proper coordination of protection. These tasks will be described in detail in the following subsections.

##### **1.5.1.2.1 Literature review**

The literature review mainly focuses on the topic of how DG integration influences the performance of the protection system in distribution networks, and what solutions are there to deal with the influence of DG integration. The major knowledge obtained from and summarized in the literature review will be introduced below.

#### **Impacts of DG integration on protection performance**

There have been quite a few research activities discussing the influence of DG integration on the distribution system protection performance in the literature. Generally, the influence exists in several manners, namely, variable fault current directions and levels, loss of protection coordination, possible islanding operation, and distribution system transient stability. Some of the main understandings with regard of these different manners are summarized in the following bullets.

- **Variable fault current directions and levels**

The traditional distribution system is usually radial in topology and the power flow as well as fault currents are single-directional. In such structure, to clear a fault requires only to open the source-end of the fault component. However, when DGs are integrated, the power flow and fault currents become bi-directional [1], while the protection system is required to open both ends of the fault component to clear a fault, although the topology of the distribution system may be not definitely meshed [2].

More discussion has focused on the fault current levels influenced by DG integration [3]. Generally, it is commonly agreed that the contribution to fault current from inverter based DGs is lower than that from directly-connected generators due to the current

limitation of inverters [4][5][6]. Normally, the converter's current during fault condition is restricted up to twice its nominal current [7]; while fault currents from synchronous generators can reach up to several times of its nominal value [8].

An example from [9] is given in Fig.1.5.1 to show the reduction of protection reach due to fault current change caused by DG integration. In Fig.1.5.1, the relay senses a smaller fault current for the same fault after DG is connected. If the settings of the overcurrent relay are not changed, the furthest fault which can be detected by the relay would be closer than the case without DG. However, the authors of [10], using hard-ware-in-the-loop simulation studies, found that DG are unlikely to cause protection reach reduction during phase to phase fault, while for single phase to earth faults, the DGs even increase the sensitivity of the protection.

Generally, DG integration makes the distribution system more complicated. The influence of DG integration on the fault current level and the reach of the network protection is dependent on many factors, such as distribution system topologies, DG type, locations and levels of DG integration, fault types, fault location, fault impedance, etc.

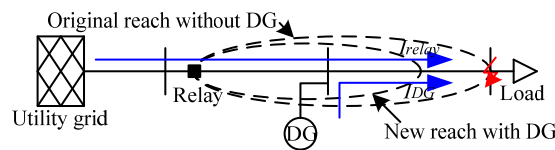


Fig.1.5.1. Reduction of protection reach

- **Loss of protection coordination**

If two devices can operate properly in the primary-backup mode when fault occurs, they are considered as in coordination [11]. However, when DGs are integrated into the distribution system, due to the varied fault current level and direction, the coordination between protection devices might be lost [7][12]. One example from [12] is given in Fig.1.5.2 to show the possibility of lost of the protection coordination. In Fig.1.5.2, no matter which occurs, fault 1 or fault 2, the fault current sensed by protection relay in bus 1 will be the same as that sensed by protection relay in bus 2. However, for fault 1, protection relay in bus 1 is supposed to operate first and protection relay in bus 2 works as the backup, while for fault 2, the other way round. This is not possible if there is only one time-current-curve setting for each of the relay and the coordination is definitely to be lost for one of the two fault cases.

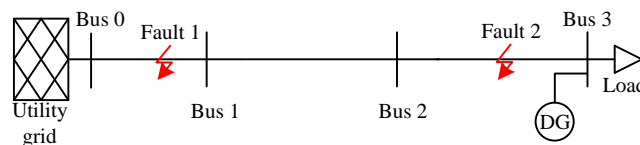


Fig.1.5.2. Loss of relay-relay coordination due to DG integration

- **Possible islanding operation**

Although IEEE 1547 standard recommends that once an island is detected, the DGs in the island should be disconnected within 2 seconds [13][14], islanding operation with DGs energizing the local loads is very likely to be an option in the future due to the reliability and flexibility it introduces [15][7]. However, the islanding operation also leads to new challenges to the protection of distribution systems.

The main cause of this challenge is that the short circuit capability of DGs is generally much lower than that can be offered by the utility grid. During islanding operation, only DGs are feeding the distribution system, thus the short circuit power and the fault currents become much lower than the grid-connected operation [16]. In this situation, the normal pickup settings of the overcurrent protection will be too high for the protection devices to operate timely when faults occur in the island [17][4][18].

- **Distribution system transient stability**

Transient stability is defined as "the ability of the power system to maintain synchronism among synchronous generators when subjected to a severe transient disturbance such as a fault on the facilities" [19]. To maintain transient stability, the protection system is required to clear the fault within a short period termed as the critical clearing time (CCT). Traditionally, transient stability is only an issue for transmission system, but not for distribution system due to its passive property.

However, the integration of DGs, e.g. directly connected synchronous generators, will add to the distribution system the transient stability problem, which may in turn bring the concept of CCT to the protection system. This is new to distribution network and would pose extra constraints on the speed of its protection devices [20][21].

### **Solutions from the DG perspective**

To mitigate the influence of DG integration on the distribution system protection, various solutions have been proposed in the literature. These solutions can be generally categorized into two groups, i.e. the solutions based on the DG technologies and the solutions embedded in the distribution network protection system. The solutions from the DG perspective are described in the following bulleted points.

- **Limit integration of DG**

This approach includes efforts in both planning and operation stages.

In the planning stage, the main concern is about how and how much DG should be integrated.

For the operation stage, solutions suggests that DG be disconnected from the distribution system during fault condition, so that the DG contribution on the fault currents will be eliminated, while the traditional protection schemes can still work without revamping the infrastructure [2]. More details about disconnecting DGs from the distribution system during fault are given in the IEEE 1547 standard [13][14]. However, as stated in [7], the tripping times in the IEEE 1547 standard are likely larger than the modern recloser operating time (6 cycles after the fault occurrence), which means the DGs will be still connected in the grid and provide fault current during the period when the recloser experiences the fault current and operates. In other words, tripping the DGs according to this standard won't help mitigate the impact of DG on protection coordination. Also as mentioned in Section I, with the increased level of DG integration, completely cutting them off during faults may cause extra problems [2]. Therefore, other alternative solutions are necessary.

- **Application of energy storage units**

The problem caused by islanding operation, i.e. much lower fault currents than grid-connected operation especially when the islanded distribution system is mainly fed by convertor-based DGs, can be solved by introducing energy storage devices which can increase fault currents so that the fault can be detected and cleared on time with protection settings for grid-connected operation [15].

The authors of [4] suggested a fly-wheel based energy storage system working together with a doubly-fed induction generator (DFIG). This combined DG unit is capable of providing sufficient fault current by injecting a controllable exponentially decaying current component, and thus the protection settings for grid-connected operation can also work properly when the system is operating in islanding mode.

- **Application of fault current limiter (FCL)**

The application of FCL has gained increasing attention in recent years. It is an effective method to reduce the fault current in power grid. Under normal condition, the impedance of FCL keeps a low value so that the power flow through it will not be affected, while under fault condition the impedance of FCL can be controlled to increase rapidly in order to reduce the fault current. In a distribution system with DGs, FCL can be used to reduce fault currents provided by the DGs, so as to keep fault current profile in the system as if no DG is integrated. Therefore the protection settings for none-DG condition can still apply, while the coordination between the protective devices can be maintained [22].

- **Novel control strategy for power-electronic based DG**

As stated in [23], with increasing integration of DG, especially those based on power electronic converters, it is important to incorporate the converter's response to a fault into fault analysis, taking into account the control strategy of the converter, the current limiting method and the fault type. This means the interaction between protection device and DG control should be taken into account when designing the power electronic converter controller. One idea proposed in [7] to mitigate the impact of inverter-based DG on recloser-fuse coordination is to modify the inverter control strategy so that during a fault, instead of completely tripping off, the inverter will reduce its output current according to its voltage deviation.

## Solutions from the protection perspective

The solutions from the protection perspective are described in the following bulleted points.

- **Improved overcurrent protection**

First of all, due to bidirectional power flow in modern distribution system caused by DG integration, conventional overcurrent protection might not satisfy the requirement, while directional overcurrent protection relays should be utilized [24].

Other contributions from the literature lie in two main aspects, i.e. the settings of the overcurrent protection devices adaptive to different operating conditions and the detection of different operating conditions. Modern micro-processor based digital protection relays allow multiple settings in one device. When multiple settings are installed in each overcurrent device, to adapt to both grid-connected and islanded conditions [17][24], or different DG integration levels [17][25][26], an appropriate way to identify different operating conditions becomes necessary in order to timely switch from one group of setting to another.

- **Other types of protection**

Although overcurrent protection is still the most commonly used protection scheme in distribution system, it meets some difficulties in identifying the fault if the fault impedance is high [27], and in clearing the fault in a short time if too many directional overcurrent relays are needed in a ring structured distribution system [28].

Therefore, other types of protection relays have been suggested for distribution system with DGs. Differential protection is used in [27] in a distribution system to improve the capability of identifying faults with low fault currents due to DG integration or high fault impedance. Distance protection is used in [28] to provide shorter fault-clearing time and it is also less sensitive to the change of fault current level and direction due to DG integration.

Furthermore, some novel protection schemes depend on neither the traditional overcurrent relays nor differential or distance relays, but the collective-knowledge based decision making stations or units. An offline-trained neural network is built in [29] and [30] to identify fault type and location, as well as to decide which one to be isolated among all those predefined protection zones. While in [31] and [32], two radial basis function neural networks were proposed to search for the fault location. The first is used to find the distance between the fault and each source; the second is to find the exact faulted line. An adaptive method is then proposed to decide which protective device should operate according to the identified fault location.

## Summarize and conclusions

Modern distribution systems are undergoing increasing penetration of DGs. Embracing the advantages that DGs bring, there are also new challenges along with this trend. One major challenge lies in the area of distribution system protection. This working task surveys the possible impacts of DG integration on distribution system protection performance and reviews the endeavors for mitigating these impacts in the literature.

The integration of DGs can impact the distribution system protection by causing variable fault current direction and level, loss of protection coordination, islanding operation, and transient stability issue.

The suggested solutions in the literature are from either the DG perspective or the protection system perspective. For the former, limiting DG integration, application of storage and FCL, modified DG control strategies are proposed to maintain the protection system performance. More solutions are proposed from the protection perspective, e.g. protection based on improved overcurrent settings, protection based on other types of relays and protection based on collective knowledge and artificial intelligence. Encountering so many options, the selection among the solutions should take into account the characteristics of the distribution system, the type and location of DG integration, and very importantly, the cost. The various solutions to the protection problem of distribution systems with DG integration, as described in the previously, are summarized in Table 1.5.1.

Table 1.5.1 Solutions for protection of distribution system with DG

Solutions	Focused problems	Advantages	Disadvantages
Limiting inte-	• Loss of protection coordination	• Provide an index for DG integration planning	• Limited utilization of DGs

gration level of DGs			
Disconnection of DGs after fault	<ul style="list-style-type: none"> <li>• Variable fault current directions and levels</li> </ul>	<ul style="list-style-type: none"> <li>• No need for updated protection system due to DG integration</li> </ul>	<ul style="list-style-type: none"> <li>• Voltage or frequency deviation because of large scale of DG cut-off</li> <li>• DG disconnection may be not fast enough for modern protection devices</li> </ul>
Application of energy storage units	<ul style="list-style-type: none"> <li>• Islanding operation</li> </ul>	<ul style="list-style-type: none"> <li>• No need for updated protection setting for islanding operation</li> </ul>	<ul style="list-style-type: none"> <li>• High cost of energy storage unit and its installation</li> </ul>
Application of FCL	<ul style="list-style-type: none"> <li>• Variable fault current directions and levels</li> </ul>	<ul style="list-style-type: none"> <li>• No need for updated protection system due to DG integration</li> </ul>	<ul style="list-style-type: none"> <li>• High cost of FCL and its installation</li> </ul>
Improved overcurrent protection	<ul style="list-style-type: none"> <li>• Variable fault current directions and levels</li> <li>• Loss of protection coordination</li> <li>• Islanding operation</li> </ul>	<ul style="list-style-type: none"> <li>• Can be updated based on existing protection system</li> </ul>	<ul style="list-style-type: none"> <li>• Methods using only local measurements may work only for small and simple distribution system</li> <li>• Methods using wide-area measurements may highly depend on ICT and thus give rise to high cost</li> </ul>
Application of differential or distance protection	<ul style="list-style-type: none"> <li>• Variable fault current directions and levels</li> </ul>	<ul style="list-style-type: none"> <li>• Adaptive to various fault current levels, high fault impedance and ring structured distribution system</li> </ul>	<ul style="list-style-type: none"> <li>• High cost of replacing the total protection system</li> </ul>
Application of collective-knowledge based decision making	<ul style="list-style-type: none"> <li>• Loss of protection coordination</li> </ul>	<ul style="list-style-type: none"> <li>• Highly adaptive to complicated multiple working conditions</li> </ul>	<ul style="list-style-type: none"> <li>• Difficult to implement</li> <li>• Highly depend on ICT and thus high cost</li> </ul>

One point to note is that, since inverter-based DGs attract more and more applications in the distribution system, the coordination between the DG control strategies and the protection mechanisms becomes a very important and promising solution. The AAU team carried out some research on DG control strategies that can assist maintaining the protection coordination during faults, and as well some research on how to cooperatively select the DG control mode and protection settings in a distribution system with multiple DGs integrated. This will be further discussed in 1.5.1.2.4.

#### **1.5.1.2.2 Modelling of the distributed generation system**

In the PRO-NET project, the AAU team built several standard test distribution system models in DIgSILENT PowerFactory 15.1 or MATLAB for simulations and method validation. These distribution system models include IEEE 13 bus test system, IEEE 33 bus test system and IEEE 34 bus test system. These models are available for the load flow calculations and time domain simulations. More details of each test system model will be introduced in next subsections where they are used in the corresponding simulations.

Some necessary modifications have been implemented in these models based on their original structure and data, in order to simulate distribution systems with DG integration. The major modification is the integration of DG unit model. A typical power electronic based DG unit, i.e. a full converter based wind turbine model, has been built and utilized for the integration with those distribution system models. This wind turbine uses a permanent magnet synchronous generator (PMSG), which is connected to the grid through a back-to-back full-scale PWM voltage source converter. This wind turbine model will be described in detail as follows.

The complete wind turbine model includes the wind speed model, the aerodynamic model of the wind turbine, the mechanical model and models of the electrical components, namely the PMSG, PWM voltage source converters, transformer, and the control system. Fig. 1.5.3 illustrates the main components of the wind turbine as well as the control system of the wind turbine.

#### **Wind speed model**

Wind speed modelling plays an important role in the study of dynamic interactions between wind farms and the connected power system. However, in small signal stability study, different operating points of the system are of concern and in each of these op-



erating points, the wind speed can be treated as a constant. Thus no detailed wind speed model is used in this work, but constant wind speeds are used.

### The aerodynamic model

The relation between the wind speed and aerodynamic torque is described by (1):

$$T_w = \frac{1}{2} \rho \pi R^3 v_{eq}^2 \frac{C_p(\theta, \lambda)}{\lambda} \quad (1)$$

where  $T_w$  is the aerodynamic torque extracted from the wind (Nm);  $\rho$  is the air density (kg/m<sup>3</sup>);  $R$  is the wind turbine rotor radius (m);  $v_{eq}$  is the equivalent wind speed (m/s);  $\theta$  is the pitch angle of the rotor (deg);  $\lambda = \omega R / v_{eq}$  is the tip speed ratio;  $\omega$  is the wind turbine rotor speed (rad/s); and  $C_p$  is the aerodynamic efficiency of the rotor.

### Mechanical model

As for the mechanical model, emphasis is put on the parts of the dynamic structure of the wind turbine that contribute to the interaction with the grid. Therefore, only the drive train is considered, while the other parts of the wind turbine structure, e.g. tower and flap bending modes, are neglected. A two-mass model is applied here to represent the drive train.

### Electrical component models

The PMSG is modelled by the synchronous generator model in DIgSILENT PowerFactory library, with a constant excitation current setting.

Since the study interest is not in the switches of the PWM converter, an average model without switches is used instead of a detailed PWM voltage source converter model so that the simulation can be carried out with relatively high calculation speed.

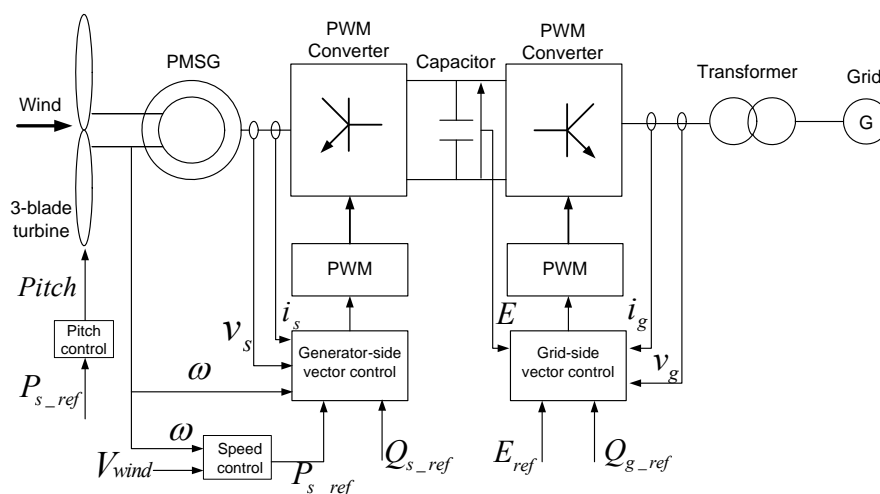


Fig. 1.5.3. Structure of the direct-drive-full-converter-based wind turbine model

### Wind turbine control system model

For a variable speed wind turbine with a PMSG and a back-to-back full-scale converter, it is possible to control the electromagnetic torque at the generator directly, so that the speed of the turbine rotor can be varied within certain limits. An advantage of the variable speed wind turbine is that the rotor speed can be adjusted in proportion to the wind speed under low to moderate wind speed condition so that the optimal tip speed ratio is maintained. At this tip speed ratio the aerodynamic efficiency,  $C_p$ , is at the maximum, which means that the energy conversion is maximized. It is normally referred to as the maximum power point tracking (MPPT) [33]. Under high wind speed condition, pitch controller as presented in Fig. 1.5.4 is activated to keep the output power at the rated value in order not to overload the system.

Vector control techniques have been well developed for PMSG using back-to-back PWM converters [34]. Two vector control schemes are designed respectively for the generator-side and grid-side PWM converters, as presented respectively in Fig. 1.5.5 and Fig. 1.5.6.

The objective of the vector-control scheme for the grid-side PWM converter is to keep the DC-link voltage constant regardless of the magnitude of the generator power, while keeping sinusoidal grid currents. It may also be responsible for controlling reactive power flow between the grid and the grid-side converter by adjusting  $Q_{g\_ref}$ . The objective of the vector-control scheme for the generator-side PWM converter is to control the optimal power tracking for maximum energy capture from the wind by adjusting the speed of the wind turbine. The reference value of the generator active power  $P_{s\_ref}$  is obtained from the rotor speed controller as shown in Fig. 1.5.7. The rotor speed reference is obtained via a look-up table to enable the optimal tip speed ratio.

Normally, the reference values of both generator-side and grid-side converters,  $Q_{s\_ref}$  and  $Q_{g\_ref}$  are set to zero to ensure unity power factor operation and reduce currents of both generator-side and grid-side converters.

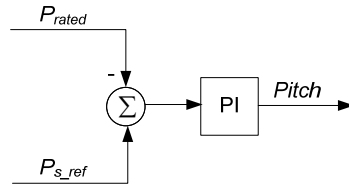


Fig. 1.5.4. Block diagram of the pitch controller

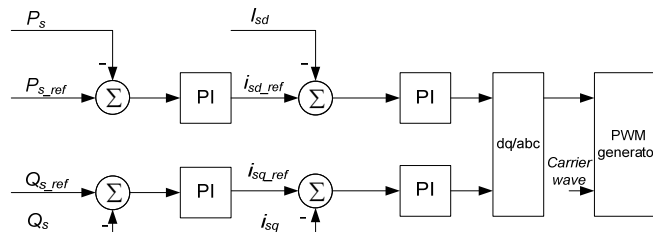


Fig. 1.5.5. Block diagram of the generator-side converter controller

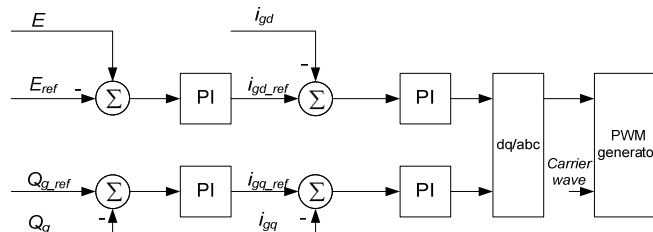


Fig. 1.5.6. Block diagram of the grid-side converter controller

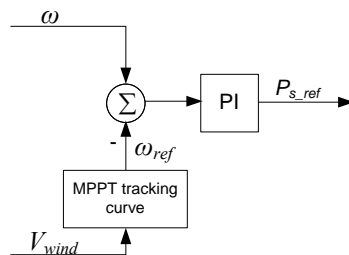


Fig. 1.5.7. Block diagram of the rotor speed controller

### 1.5.1.2.3 Short circuit analysis of distribution systems with DG integration

DG integration may change the pattern of the fault currents in the distribution system and as a result bring challenges to the network protection system. This problem has been frequently discussed in the literature, but mostly considering only the balanced fault situation. In the PRO-NET project, the AAU team presents an investigation on the influence of full converter based wind turbine (WT) integration on fault currents during both balanced and unbalanced faults. Major factors such as external grid short circuit power capacity, WT integration location, connection types of WT integration transformer are taken into account. The investigation is based on mathematical analysis and simulation study of a simple test system built in DIgSILENT PowerFactory. The protection is-

sues as a result of the change of fault current after DG integration are presented as well.

### Mathematical analysis

The test system is shown in Fig.1.5.8, which is a simple system for the purpose of clearly presenting the impacts of DG integration on short circuits during different types of faults. This test system includes three buses, namely, the feeder beginning bus which interfaces the feeder with the external power grid, the PCC bus where the DG unit is integrated, and the load bus. Two protection devices P1 and P2 are installed respectively at the interface bus and the PCC bus. The connection type of the transformer T1 is selected as delta-YN (delta at the external grid side). The connection type of the transformer T2 has two options in the following study, i.e. YN-YN connection and YN-delta connection (delta at the test system side). The basic data of the test feeder is presented in Table 1.5.2.

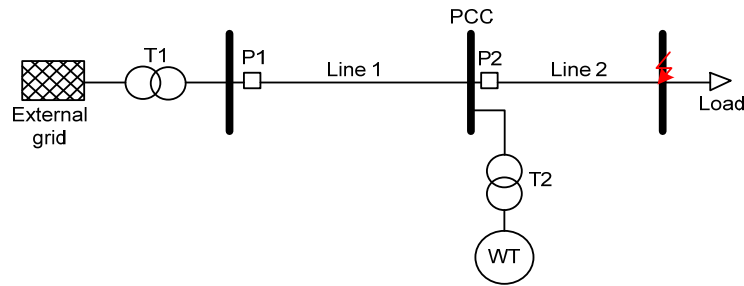


Fig.1.5.8. Test system with wind turbine connected

Table 1.5.2. Basic Data of the Test Feeder

Nominal voltage (kV)	24.9
Line resistance ( $\Omega$ /mile)	1.34
Line reactance ( $\Omega$ /mile)	1.33
Length of line1: beginning to PCC (mile)	7.1
Length of line2: PCC to load bus (mile)	5.6
Short circuit capacity of the external grid (MVA)	10
Load capacity (MW)	1.0
AC system frequency (Hz)	50

Because of the fact that the single phase to ground short circuit is the most frequent type of fault, while the three phase short circuit is considered as the most severe fault in the power system, these two types of faults are selected in this study to represent respectively unbalanced fault and balanced fault.

Suppose a three phase short circuit occurs at the load bus in Fig.1.5.8. The equivalent circuits during this fault of the test system with and without WT integration are given in Fig.1.5.9.

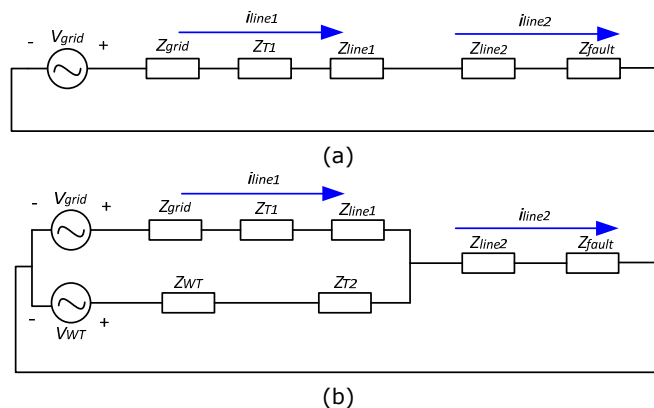


Fig.1.5.9. Equivalent circuits of the test system during three phase short circuit fault: (a) equivalent circuit without WT; (b) equivalent circuit with WT

In Fig.1.5.9,  $Z_{grid}$  and  $Z_{WT}$  are respectively the inner impedance of the external grid and the WT unit. For simplicity, an assumption is that  $V_{WT}$  equals to  $V_{grid}$ , which are both equal to  $V$ . Given  $Z_i = Z_{grid} + Z_{T1} + Z_{line1}$ ,  $Z_j = Z_{line2} + Z_{fault}$  and  $Z_k = Z_{WT} + Z_{T2}$ , the currents during three phase fault without WT integration are obtained in (2).

$$i_{time1} = i_{time2} = \frac{V}{Z_i + Z_j} \quad (2)$$

While the currents during three phase fault with WT integration are obtained in (3) and (4).

$$i_{time2} = \frac{V}{Z_i || Z_k + Z_j} \quad (3)$$

$$i_{time1} = \frac{V}{Z_i || Z_k + Z_j} * \frac{Z_k}{Z_i + Z_k} = \frac{V}{Z_i + Z_j + \frac{Z_i Z_j}{Z_k}} \quad (4)$$

It can be observed that, when WT is integrated, the total fault current at the fault location would increase ((3) compared with (2)), while the fault current from the upstream external grid would decrease ((4) compared with (2)).

Single phase to ground fault is unbalanced, which requires to use symmetrical component method to analyze the fault current. Since it is normal to use zero sequence current in the ground fault protection during a single phase to ground fault, the zero sequence current is the main focus for the analysis of single phase fault.

The zero sequence total fault current during a single phase to ground fault is given in (5).

$$i_0 = \frac{3V}{Z_{1\Sigma} + Z_{2\Sigma} + Z_{0\Sigma}} \quad (5)$$

In (5),  $Z_{1\Sigma}$ ,  $Z_{2\Sigma}$  and  $Z_{0\Sigma}$  are respectively the equivalent positive sequence impedance, equivalent negative sequence impedance and equivalent zero sequence impedance, which can be calculated in corresponding sequence networks [35].

The positive sequence and the negative sequence networks of the test system are in the same pattern as the circuits in Fig. 1.5.9, except for the voltage source which doesn't influence the impedance calculation. Therefore, the equivalent positive sequence impedance  $Z_{1\Sigma}$  and the equivalent negative sequence impedance  $Z_{2\Sigma}$  of the test system without and with WT integration are represented by (6) - (9) respectively.

For test system without WT:

$$Z_{1\Sigma} = Z_{1t} + Z_{1f} \quad (6)$$

$$Z_{2\Sigma} = Z_{2t} + Z_{2f} \quad (7)$$

For test system with WT integration:

$$Z_{1\Sigma} = Z_{1t} || Z_{1k} + Z_{1f} \quad (8)$$

$$Z_{2\Sigma} = Z_{2t} || Z_{2k} + Z_{2f} \quad (9)$$

In (6)-(9), the impedances  $Z_{1i}$ ,  $Z_{1j}$ ,  $Z_{1k}$  and  $Z_{2i}$ ,  $Z_{2j}$ ,  $Z_{2k}$  are defined in the similar way to  $Z_i$ ,  $Z_j$ ,  $Z_k$  for the three phase fault study. Apparently, the values of  $Z_{1\Sigma}$  and  $Z_{2\Sigma}$  decrease when WT is integrated.

Zero sequence network of the test system is more special, which in the case of WT integration strongly depends on the type of connection of the interface transformer T2. As mentioned previously, two connection types of T2 are considered and compared in this paper, i.e. YN-YN connection and YN-delta connection (delta at the system side). The equivalent zero sequence network of the test system without WT, with WT (YN-delta) and WT (YN-YN) are demonstrated in Fig.1.5.10.

In Fig. 1.5.10,  $V_0$  denotes the equivalent zero sequence voltage source at the fault location [35]. Because all the three phase zero sequence currents pass through it, the fault impedance is taken as three times the original value in these equivalent circuits. It can be observed in Fig.1.5.10 that the zero sequence equivalent circuit with WT (YN-delta) is the same as the one without WT. This is due to the fact that zero sequence current cannot pass through delta connection. For the same reason (T1 is delta connection at the external grid side), the inner impedance of the external grid is not in the zero se-

quence circuit either. For YN-YN connection, the WT branch is included in the zero sequence equivalent circuit. Here define  $Z_{0i} = Z_{0T1} + Z_{0line1}$ ,  $Z_{0j} = Z_{0line2} + 3*Z_{0fault}$  and  $Z_{0k} = Z_{0WT} + Z_{0T2}$ , and the equivalent zero sequence impedance  $Z_{0\Sigma}$  can be obtained by (10) and (11).

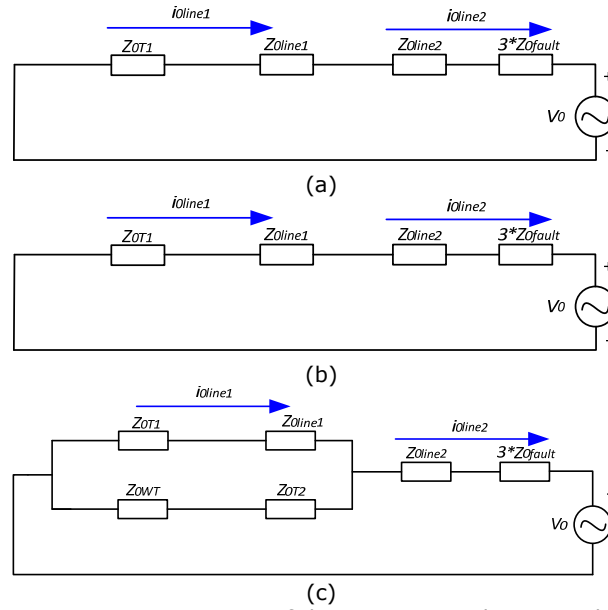


Fig.1.5.10. Equivalent zero sequence circuits of the test system during single phase to ground short circuit fault: (a) without WT; (b) with WT (YN-delta), (c) with WT (YN-YN)

For test system without WT or with WT (YN-delta):

$$Z_{0\Sigma} = Z_{0k} + Z_{0j} \quad (10)$$

For test system with WT (YN-YN):

$$Z_{0\Sigma} = Z_{0k} || Z_{0k} + Z_{0j} \quad (11)$$

Thus with WT integrated, the equivalent zero sequence impedance would keep unchanged if the WT transformer is YN-delta connection; while the zero sequence impedance would decrease if the WT transformer is YN-YN connection.

Consequently, according to (5), the total zero sequence fault current  $i_{0line2}$  would increase with WT integrated to the test system, because integration of WT decrease the equivalent positive sequence impedance  $Z_{1\Sigma}$  and the equivalent negative sequence impedance  $Z_{2\Sigma}$ . Plus,  $i_{0line2}$  would increase even more if the WT is connected through YN-YN transformer, because this connection can lead to decrease of the equivalent zero sequence impedance  $Z_{0\Sigma}$ , while YN-delta connection can not.

For the fault current from the grid side  $i_{0line1}$ , it increases identically with the total fault current  $i_{0line2}$  if the WT is connected through YN-delta transformer; while it would decrease if the WT is connected through YN-YN transformer, because as shown in Fig.1.5.10 (c),  $i_{0line1}$  becomes only a fraction of  $i_{0line2}$  in this case.

### Simulation results

The instantaneous fault current from the external grid side ( $i_{line1}$ ) and the total fault current ( $i_{line2}$ ) during a three phase short circuit (occurring at 50s) are respectively given in Fig.1.5.11 and Fig.1.5.12.

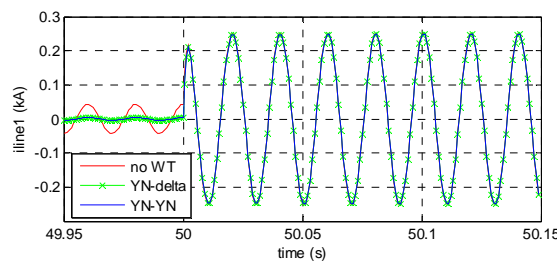


Fig.1.5.11. Fault current from the external grid side during a three phase short circuit fault

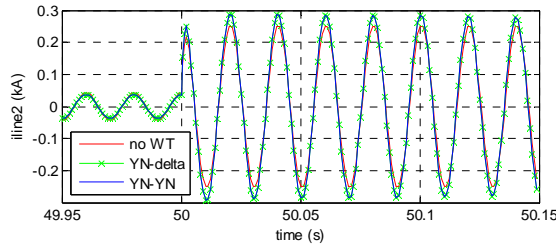


Fig.1.5.12. Total fault current during a three phase short circuit fault

The different connection types of the WT integration transformer do not cause difference in the fault currents in Fig.1.5.11 or Fig.1.5.12. During a three phase short circuit fault, with WT integrated through either transformer type, the fault current from the external grid decreases, and the total fault current increases. This is consistent with the mathematical analysis.

To further validate the mathematical analysis for three phase fault, the change of WT location and the change of the external grid SC power are taken into account. The location of the WT is changed by varying the length of line1 and line2, while keeping their total length at 12.7 miles as given in Table 1.5.1. The SC power is changed within the range between 6MVA and 25MVA by varying the value of  $Z_{grid}$ .

The change of the RMS values of the three phase short circuit fault current with respect to the length of line1 is illustrated in Fig.1.5.13 and Fig.1.5.14, respectively the external grid side fault current and the total fault current.

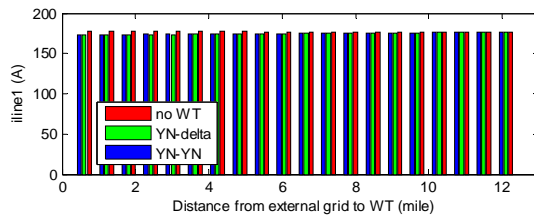


Fig.1.5.13. RMS value of the external grid side fault current with respect to the distance from the external grid to the WT (three phase short circuit fault)

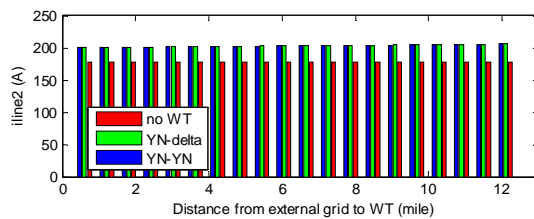


Fig.1.5.14. RMS value of the total fault current with respect to the distance from the external grid to the WT (three phase short circuit fault)

The change of the RMS values of the three phase short circuit fault current with respect to the external grid SC power is illustrated in Fig.1.5.15 and Fig.1.5.16, respectively the external grid side fault current and the total fault current.

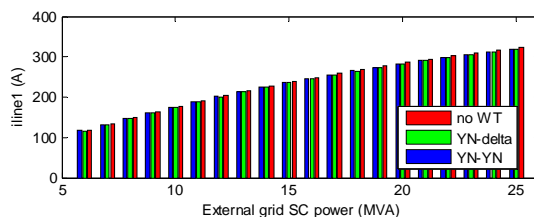


Fig.1.5.15. RMS value of the external grid side fault current with respect to the SC power of the external grid (three phase short circuit fault)

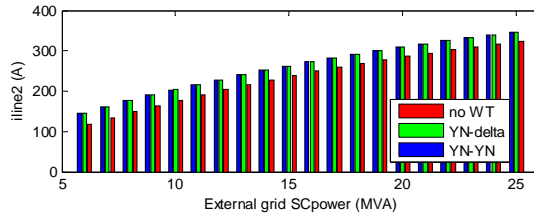


Fig.1.5.16. RMS value of the total fault current with respect to the SC power of the external grid (three phase short circuit fault)

From Fig.1.5.13 – Fig.1.5.16, it is apparent that the location of WT integration has minor influence on either the fault current from the grid side or the total fault current; while the external grid SC power has much stronger influence. This is because as show in Fig.1.5.9, changing the external grid SC power is to change the value of  $Z_{grid}$ , which has a major impact on the total impedance for the short circuit current calculation; while changing the location of WT is to change the values of  $Z_{line1}$  and  $Z_{line2}$  but their sum keeps unchanged, which has much less impact on the total impedance for the short circuit current calculation.

The instantaneous zero sequence fault current from the external grid side ( $i_{line1}$ ) and the total fault current ( $i_{line2}$ ) during single phase to ground short circuit fault are respectively given in Fig.1.5.17 and Fig.1.5.18.

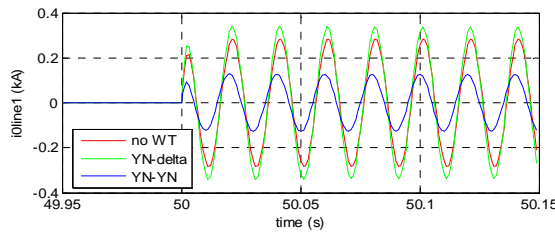


Fig.1.5.17. Zero-sequence fault current from the external grid side during single phase to ground short circuit fault

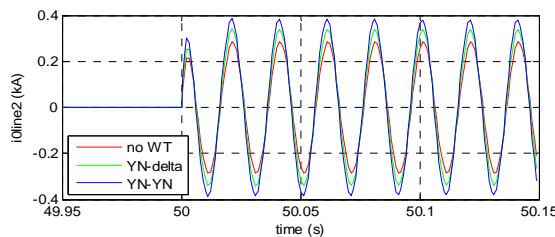


Fig.1.5.18. Total zero-sequence fault current during single phase to ground short circuit fault

In Fig.1.5.18, as expected from the mathematical analysis, the total fault current during a single phase to ground fault increases when WT is integrated, and the YN-YN connection can lead to larger increase than the YN-delta connection. For the fault current from the external grid side in Fig.1.5.17, it increases if WT is integrated through YN-delta connection, and decreases if WT is integrated through YN-YN connection, which is also consistent with the mathematical analysis for single phase fault.

The change of the RMS values of the zero sequence fault current (during single phase to ground fault) with respect to the length of line1 is illustrated in Fig.1.5.19 and Fig.1.5.20, respectively the external grid side fault current and the total fault current.

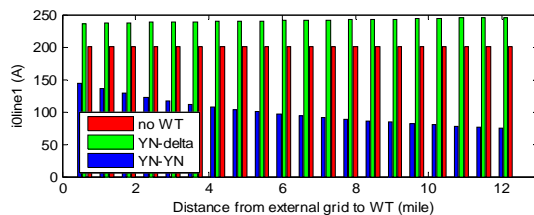


Fig.1.5.19. RMS value of the external grid side zero sequence fault current with respect to the distance from the external grid to the WT (single phase to ground short circuit fault)

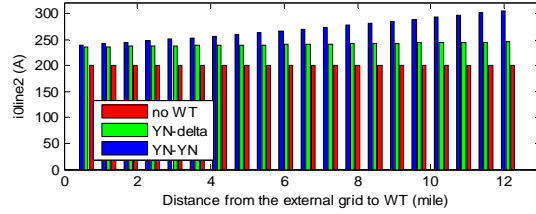


Fig.1.5.20. RMS value of the total zero sequence fault current with respect to the distance from the external grid to the WT (single phase to ground short circuit fault)

The change of the RMS values of the zero sequence fault current (during single phase to ground fault) with respect to the SC power of the external grid is illustrated in Fig.1.5.21 and Fig.1.5.22, respectively the external grid side fault current and the total fault current.

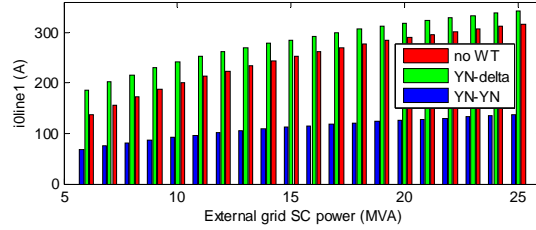


Fig.1.5.21. RMS value of the external grid side zero sequence fault current with respect to the SC power of the external grid (single phase to ground short circuit fault)

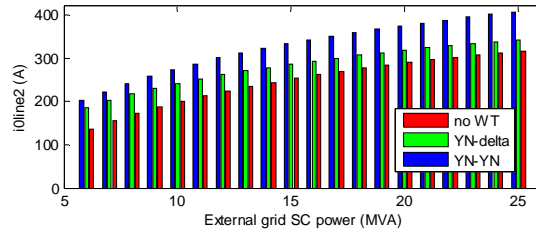


Fig.1.5.22. RMS value of the total zero sequence fault current with respect to the SC power of the external grid (single phase to ground short circuit fault)

In Fig.1.5.19 and Fig.1.5.20, the location of the WT integration can noticeably influence the fault current during single phase to ground fault only when the WT is connected through YN-YN type transformer. The explanation is as follows. Firstly, according to the mathematical analysis, the change of  $Z_{line1}$  and  $Z_{line2}$  cannot influence any of  $Z_{1\Sigma}$ ,  $Z_{2\Sigma}$  and  $Z_{0\Sigma}$  when no WT is integrated, because the sum of  $Z_{line1}$  and  $Z_{line2}$  is not changed. If WT is connected through YN-delta transformer,  $Z_{1\Sigma}$  and  $Z_{2\Sigma}$  would slightly decrease along with the increase of  $Z_{line1}$  and decrease of  $Z_{line2}$ ; while  $Z_{0\Sigma}$  would not change, so only slight increase of fault current can be observed in Fig.1.5.19 and Fig.1.5.20 (the green bars). For YN-YN connection,  $Z_{1\Sigma}$ ,  $Z_{2\Sigma}$  and  $Z_{0\Sigma}$  all decrease with the increase of  $Z_{line1}$  and decrease of  $Z_{line2}$ , so the total fault current increases more drastically (blue bars in Fig.1.5.20); while the fault current from the external grid side decrease (blue bars in Fig.1.5.19) due to the increasing impedance of its circuit branch.

Regarding the increase of the SC power of the external grid (in other words, decrease of  $Z_{grid}$ ), no matter WT is integrated or not, it can decrease  $Z_{1\Sigma}$  and  $Z_{2\Sigma}$  while barely influence  $Z_{0\Sigma}$ , so both fault current from the external grid side and the total fault current increase in all cases as shown in Fig.1.5.21 and Fig.1.5.22.

Over current protection relay and zero sequence over current protection relay are respectively used for the test system protection during three phase short circuit fault and single phase to ground short circuit fault. Current time characteristics "IAC Short Inverse GES7003A" and "IAC Very Inverse GES7002B" in DIgSILENT library are respectively selected for the over current and zero sequence over current protection.

Fault occurs at the load bus, thus P2 in Fig.1.5.8 serves as the main protection, while P1 is the backup protection.

The fault impedance range is selected based on the study in [36]. Specifically, 0-10 $\Omega$  is selected for the three phase fault, and 0-190 $\Omega$  is selected for the single phase to ground fault. Thus, to detect the maximum fault impedance at the load bus, the pickup current



and time dial settings of the main and backup protection for both types of faults are obtained and listed in Table 1.5.3.

The protection settings in Table 1.5.3 are selected for the test system without WT integration. When WT is integrated, since the fault current may be different, the performance of the protection device can be influenced. The operation time of the main protection and the backup protection are obtained for cases with and without WT integration through time domain simulation in DIgSILENT PowerFactory and listed in Table 1.5.4 and Table 1.5.5, respectively for three phase fault and single phase to ground fault.

Table 1.5.3. Protection Settings

	Three phase fault		Single phase fault	
	P2(Main)	P1(Backup)	P2(Main)	P1(Backup)
Pickup current (A)	112.5	112.5	30	30
Time dial	5	2	1	0.5

Table 1.5.4. Protection Performance during Three Phase Fault

	No WT		WT (YN-delta)		WT (YN-YN)	
	0	10	0	10	0	10
$Z_{fault} (\Omega)$	0	10	0	10	0	10
Operation time of P2 (s)	0.251	0.306	0.221	0.250	0.221	0.250
Operation time of P1(s)	0.599	0.733	0.606	No operation	0.606s	No operation

Table 1.5.5. Protection Performance during Single Phase Fault

	No WT		WT (YN-delta)		WT (YN-YN)	
	0	190	0	190	0	190
$Z_{fault} (\Omega)$	0	190	0	190	0	190
Operation time of P2 (s)	0.110	1.46	0.097	0.880	0.091	0.778
Operation time of P1(s)	0.210	2.90	0.191	1.74	0.565s	No operation

Since WT integration increases the total fault current while decreases the fault current from the external grid side during three phase fault, the operation time decreases for the main protection (P2) but increases for the backup protection (P1). When the fault impedance is at the maximum (10 $\Omega$ ), the backup protection cannot detect the fault with WT integrated, while the new maximum detectable fault impedance is 8 $\Omega$ .

With regard to single phase fault, WT (YN-delta) integration increases both fault currents, so the operation time of P2 and P1 both decreases, while the new maximum detectable fault impedance is 238 $\Omega$ . While WT (YN-YN) increases the total fault current while drastically decreases the fault current from the external grid, thus the operation time decreases for P2 but increases for the P1. When the fault impedance is at the maximum (190 $\Omega$ ), the backup protection cannot detect the fault, while the new maximum detectable fault impedance is 50 $\Omega$ .

In general, for three phase fault, WT integration improves the sensitivity of the downstream protection device, while reduce the sensitivity of the upper-stream protection device. While for single phase fault, the influence strongly depends on the connection type of the WT integration transformer.

## Conclusion

This study mathematically investigates the influence of WT integration on fault currents during two typical types of faults, and two connection types of the integration transformer are compared. For three phase fault, the connection type of the WT transformer doesn't matter. Generally, the downstream fault current increases while the upstream

fault current decrease. During single phase fault, the influence depends on the WT transformer connection type. These conclusions have been validated by fault current and protection performance results obtained through time domain simulation in DIG-SILENT.

#### 1.5.1.2.4 DG control strategies during fault

As before mentioned, DG integration in distribution system could change the short circuit current profile during faults and thus create impacts on the coordination of protection devices. As a protection measure commonly used in distribution network, recloser-fuse coordination could suffer from this impact. This problem can be solved by both changing the protection settings and changing the DG control mode during faults. In the PRO-NET project, the AAU team mainly focuses on the latter. Previous research work has been conducted to deal with this problem by modifying the control strategy of the DG converters during faults. These solutions generally reduce the current output from the converters during faults so as to mitigate the influence on protection coordination. However, converter current reduction may not be necessary for all types of faults. In the PRO-NET project, the AAU team proposes a converter control which is adaptive to different fault types and also non-fault voltage drop events. This control strategy is validated by simulations in DIGSILENT PowerFactory.

#### Problem and previous solution

In the test feeder shown in Fig.1.5.23, a recloser is installed at the beginning of the feeder, while a fuse is installed at a downstream section. A DG unit is integrated at the PCC bus between the recloser and the fuse.

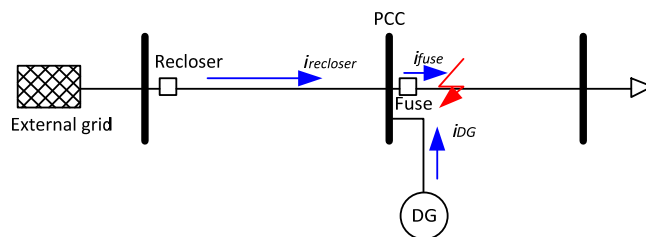


Fig.1.5.23. Simplified test system with a recloser and a fuse installed

With fuse-saving method, if a fault occurs at a location as denoted in Fig. 1.5.23, the recloser should trip first and then reclose after a predefined period. If the fault still exists (i.e. a long term or permanent fault), the fuse should melt, otherwise (i.e. a temporary fault) the feeder restores its operation. This fuse saving coordination is realized by selecting proper time-current curves for the two protection devices. As shown in Fig. 1.5.24, the maximum fault current when there is no DG is denoted by the red dashed line. It can be seen, for any possible fault current value without DG, the fuse curve is above the recloser curve, which means the recloser will trip first during faults and the protection coordination is achieved. However, if DG is integrated as shown in Fig. 1.5.23, the fault current sensed by the recloser will be reduced, while the fault current sensed by the fuse will be increased. If a maximum short-circuit fault occurs under this condition, the recloser operation time can be longer than the fuse melting time as denoted by the yellow and green dashed lines in Fig. 1.5.24 (i.e.  $t_{recloser} > t_{fuse}$ ). In other words, the coordination between the recloser and the fuse is collapsed.

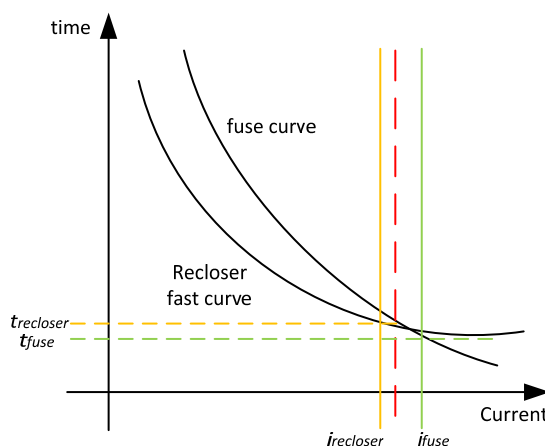


Fig.1.5.24. Recloser and fuse coordination lost

To solve this problem, a control strategy of DG converter has been proposed in [7]. It uses the PCC voltage as an indicator. Once the PCC voltage decreases below 0.88p.u, the converter output current is reduced according to (11). In (11),  $n$  is a constant that determines the sensitivity of the control strategy to the PCC voltage drop during faults; while  $k$  is determined by (12) after  $n$  has been selected.  $P_{desired}$  is the desired output power of the DG.

$$I_{ref} = k * V_{PCC}^n \text{ if } V_{PCC} < 0.88 \text{ p.u} \quad (11)$$

$$k * 0.88^n = \frac{P_{desired}}{V_{PCC}^n} \quad (12)$$

This method has been proved to be effective in maintaining the coordination of recloser and fuse in [7]. However, one fact is that it may not always be necessary to reduce the current from DG during a fault. For example, if a high impedance short circuit occurs at the location as shown in Fig. 1.5.23, the fault current without DG is denoted by the red dashed line in Fig. 1.5.25. In this case, even if DG is integrated, the coordination of the recloser and the fuse can still be maintained, though the fault current sensed by the recloser decreases and the fault current sensed by fuse increases (as denoted by the yellow and green lines in Fig. 1.5.25). Therefore, in this case, there is no need to decrease the DG current output, although the PCC voltage will very probably decrease below 0.88p.u during this high impedance short circuit fault.

Another issue with this strategy is that some non-fault events (e.g. load event) can also lead to a PCC voltage lower than 0.88p.u. Although this is not the case where the output current of the DG should be decreased, this method will activate the current-reducing control of the DG converter during the event any way.

In summary, with only PCC voltage as an indicator to activate the current-reducing control for DG converters during events may be too conservative. DG integration does not necessarily cause recloser-fuse mis-coordination during all low PCC voltage events.

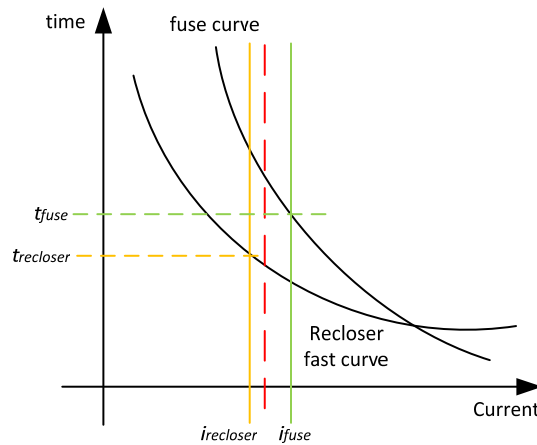


Fig. 1.5.25. Recloser and fuse coordination maintained during high impedance fault

### Proposed solution

Since PCC voltage is not sufficient to distinguish different events as explained in the previous section, the adaptive control strategy proposed in the PRO-NET project by the AAU team includes the downstream current (i.e. the current sensed by the fuse) from the PCC as the second indicator.

As shown in Fig.1.5.26, the axis of current is divided into three sections by the two red dashed lines. For all the events with PCC voltage lower than 0.88p.u, if the fuse current is higher than  $i_1$ , it is considered as a low-impedance fault event which presents high risk of recloser-fuse mis-coordination; if the fuse current is between  $i_2$  and  $i_1$ , it is considered as a high-impedance fault event and there is no risk for loss of recloser-fuse coordination; while if the fuse current is below  $i_2$ , the event is considered as a load event in no need of protection actions at all. The values of  $i_1$  and  $i_2$  may vary among different distribution feeders, and should be determined by fault calculation and simulation tests.

Therefore, the control logic of the proposed adaptive control strategy is given in equation (13). For normal operation ( $V_{PCC} \geq 0.88 \text{ p.u}$ ), the converter current is controlled to

generate the desired power from the DG. For low impedance fault events, the converter current is reduced as in [7], according to the PCC voltage drop, in order to maintain coordination between recloser and fuse. For high impedance fault events, the converter current is controlled in the same way as the normal operation, because the recloser-fuse coordination is not threatened by the DG integration. For non-fault load events, PCC voltage control should be activated in the DG converter to contribute to the voltage support in the distribution network.

$$\begin{cases} I_{ref} = \frac{P_{desired}}{V_{PCC}}, \text{ IF } V_{PCC} \geq 0.88 \text{ p.u.} \\ I_{ref} = k * V_{PCC}, \text{ IF } V_{PCC} < 0.88 \text{ p.u. and } t_{fuse} > t_1 \\ I_{ref} = \frac{P_{desired}}{V_{PCC}}, \text{ IF } V_{PCC} < 0.88 \text{ p.u. and } t_2 < t_{fuse} < t_1 \\ \text{PCC voltage control is activated, IF } V_{PCC} < 0.88 \text{ p.u. and } t_{fuse} < t_2 \end{cases} \quad (13)$$

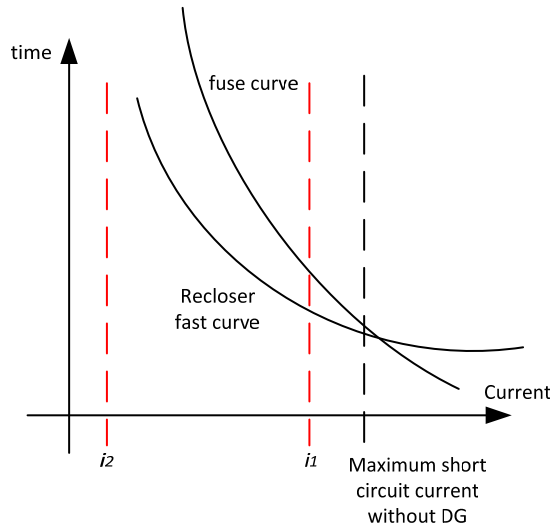


Fig.1.5.26. Use current to decide control strategy

### Case study and simulation results

The DG unit in the test feeder is modelled as a full converter-based wind turbine which has been introduced in 1.5.1.2.2. The control strategy given in [7] and the proposed adaptive control strategy are respectively implemented in the grid-side converter controller of the wind turbine. The performance of these two control strategies under various conditions are simulated and compared.

The time current curves presented in Fig. 1.5.27 of the recloser and the fuse are selected. The curves intersect at a point to the right of the maximum fault current so that the recloser-fuse coordination can be achieved.

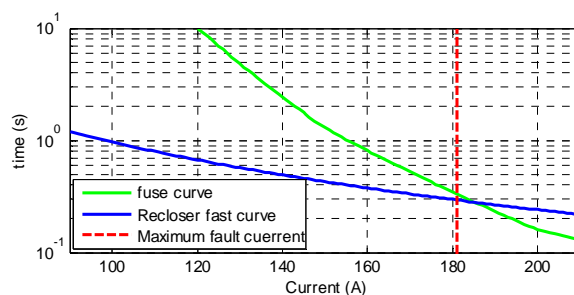


Fig.1.5.27. Time-current curves of the recloser and the fuse in the test feeder

The full-converter based wind turbine is rated at 500kW. Regarding the control strategies discussed in this paper, the grid-side converter controller is on the focus. The diagram of the grid-side converter controller is illustrated in Fig.1.5.28.

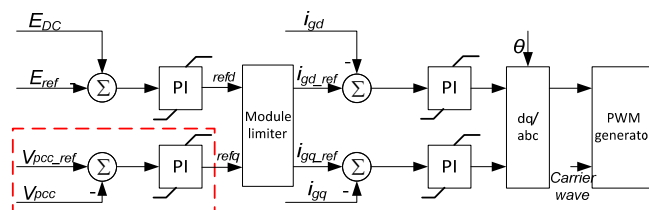


Fig.1.5.28. Diagram of the grid-side converter controller for the full-converter based wind turbine

Vector control schemes are used in the grid-side converter controller, so that the output active power and reactive power can be separately controlled. Instead of reactive power control as shown in Fig.1.5.6, a PCC voltage controller is embedded in the q-axis part of the grid-side converter controller as in the red frame in Fig. 1.5.28.

Three study cases are taken into account:

Case 1 - the low impedance fault ( $0\Omega$ ) case,

Case 2 - the high impedance ( $24+j18\Omega$ ) fault case,

Case 3 - the load increase (0.9MVA ramp in 1s) event with voltage drop (to below 0.88p.u) case.

The two control strategies are separately implemented in the module limiter within the grid-side converter controller of the wind turbine. For the proposed strategy, the q-axis current reference is limited to zero in most situations, so as to maintain a high power factor of the converter output; while during the load event with a severe voltage drop, the PCC voltage controller is activated and the q-axis current reference can have a value higher than zero and be limited in combination with the d-axis current reference. The rated current of the feeder is 30A, while the values of  $i_1$  and  $i_2$  are respectively selected by tests as 60A (2.0 p.u.) and 150A (5.0 p.u.) for the test feeder in this paper.

The short-circuit fault events in case 1 and case 2 occur at 35s during the time simulation in the location shown in Fig.1.5.23. The load event in case 3 also occurs at 35s in the load model of the feeder. The wind turbine is working at its rated power.

Case 1 - low impedance fault:

The currents sensed by the recloser and the fuse in case 1 are respectively presented in Fig. 1.5.29 and Fig. 1.5.30. The recloser and the fuse behavior in case 1 are shown in Fig. 1.5.31 and Fig. 1.5.32, in which value '0' denotes the tripping state of the protection device, while value '1' denotes the normal connection.

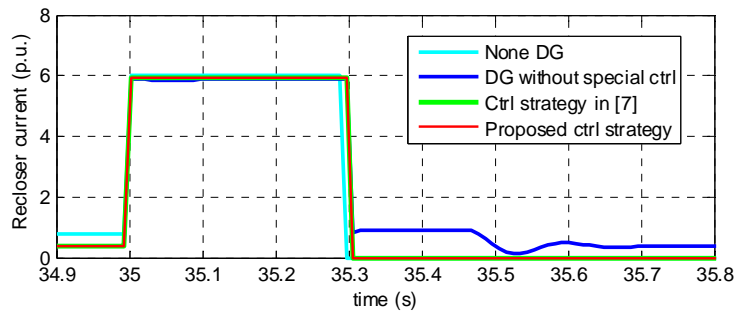


Fig.1.5.29. Recloser current in case 1

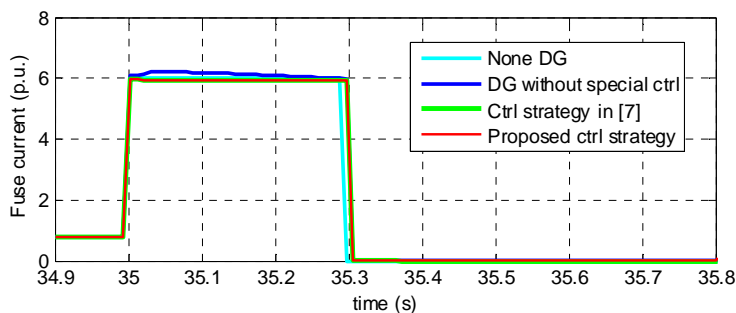


Fig.1.5.30. Fuse current in case 1

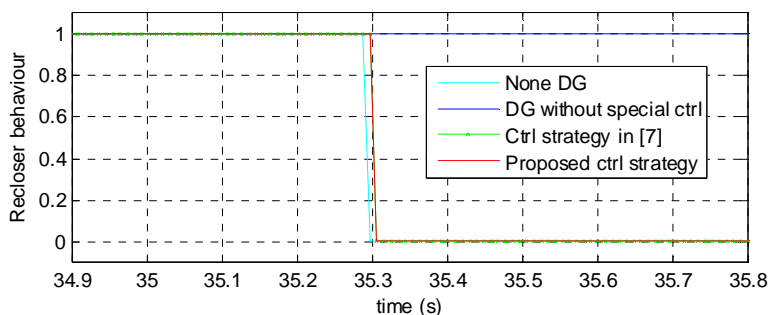


Fig.1.5.31. Recloser behaviour in case 1

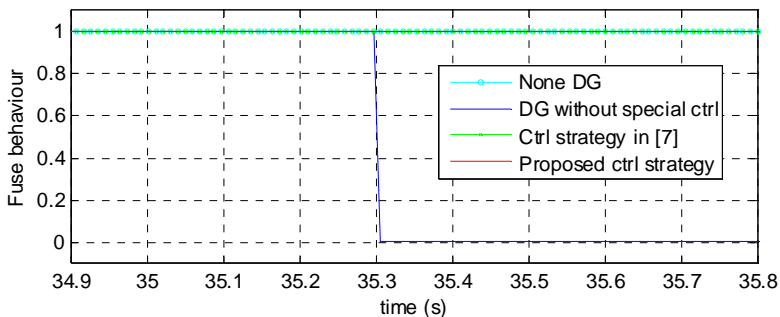


Fig.1.5.32. Fuse behaviour in case 1

Since the event in case 1 is a short circuit with zero fault impedance, the fault current without DG is at the maximum value (181A, i.e. around 6.0 p.u.). When the DG is integrated (the dark blue curves), the recloser current decreases and the fuse current increases compared with the none-DG situation (the light blue curves). This is a dangerous situation for the recloser-fuse coordination, which is proven so in Fig. 1.5.31 and Fig. 1.5.32 that the fuse melts before the recloser can act when the DG is integrated.

When either the control strategy in [7] (the green curves) or the proposed control strategy (the red curves) is implemented in the DG, the recloser current and the fuse current can be kept very close to the value without DG, thus the recloser-fuse coordination is maintained. As in Fig. 1.5.31 and Fig. 1.5.32, for either of the two control strategies, the recloser trips the feeder shortly after the fault occurs, without fuse melting.

This study case verifies the effectiveness of the two control strategies in mitigating the negative influence of DG integration on the recloser-fuse coordination.

Case 2 - high impedance fault:

The currents sensed by the recloser and the fuse in case 2 are respectively given in Fig. 1.5.33 and Fig. 1.5.34. The recloser and the fuse behavior in case 2 are shown in Fig. 1.5.35 and Fig. 1.5.36.

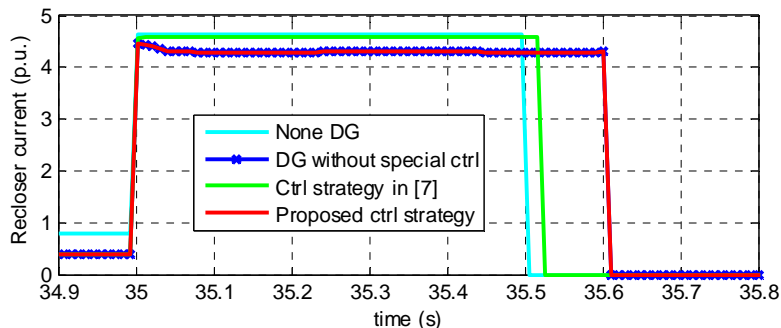


Fig.1.5.33. Recloser current in case 2

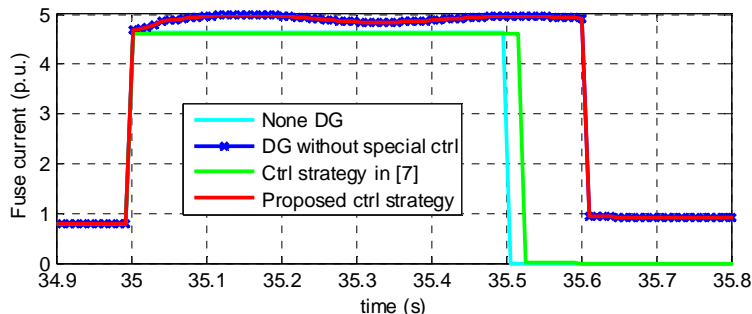


Fig.1.5.34. Fuse current in case 2

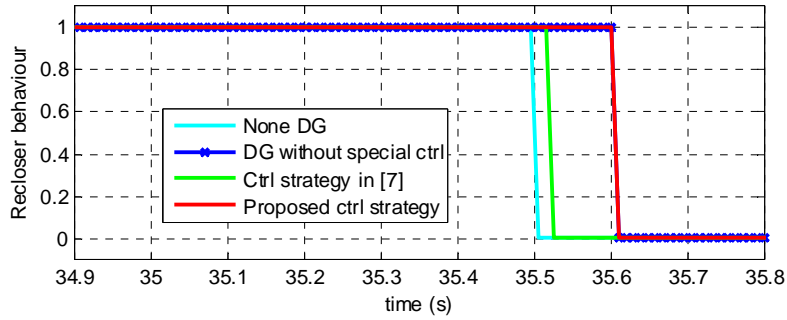


Fig.1.5.35. Recloser behaviour in case 2

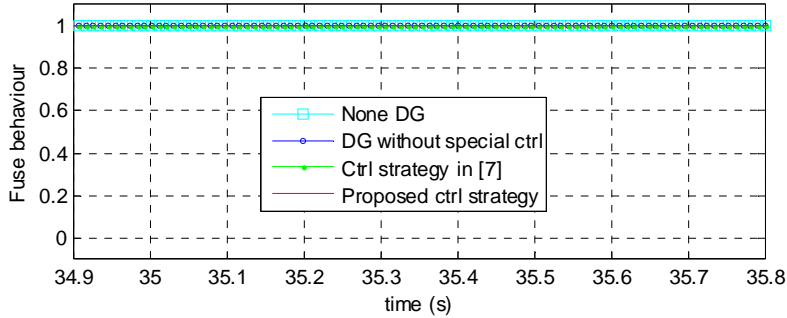


Fig.1.5.36. Fuse behaviour in case 2

The event in case 2 is a high impedance fault. As explained previously, DG integration under this situation can rarely devastate the recloser-fuse coordination. Accordingly, as indicated by the above figures, although DG integration can decrease the recloser current while increase the fuse current, the recloser acts without fuse melting, i.e. the recloser-fuse coordination is maintained.

Comparing the two control strategies, the strategy in [7] takes action during the fault to mitigate the contribution of DG on the fault current, because the PCC voltage drops below 0.88 p.u.; while the proposed strategy takes no special action during the fault because the fuse current is in the range between  $i_1$  and  $i_2$ . Using either strategy, the recloser-fuse coordination is maintained, which is also demonstrated in Fig. 1.5.35 and Fig. 1.5.36.

However, these two control strategies influence the wind turbine operation during fault in different ways. Specifically, as presented in Fig. 1.5.37, the proposed control strategy allows smoother wind power generation during fault than the control strategy in [7], and thus as presented in Fig. 1.5.38, the wind turbine DC link voltage rise during fault is much less than the control strategy in [7]. In other words, the proposed control strategy provides a more tender condition during high-impedance fault for the wind turbine to ride through. Note that no special control scheme for fault-ride-through (which is beyond the scope of the study) in the generator side convertor and the DC link circuit of the wind turbine has been implemented in this study cases, and thus the DC voltage increase shown in Fig.1.5.38 represents a possibility instead of the real case.

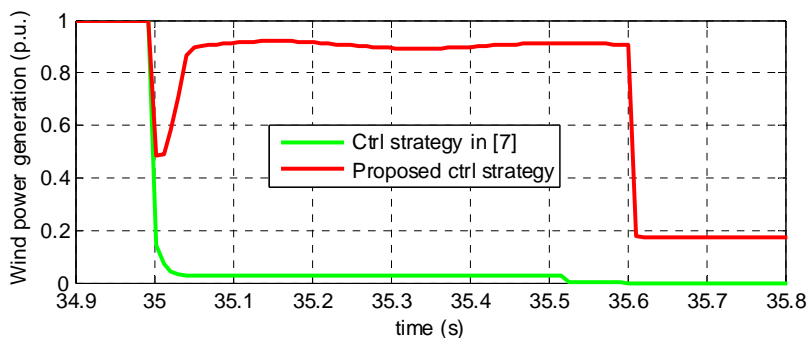


Fig.1.5.37. Wind power generation in case 2

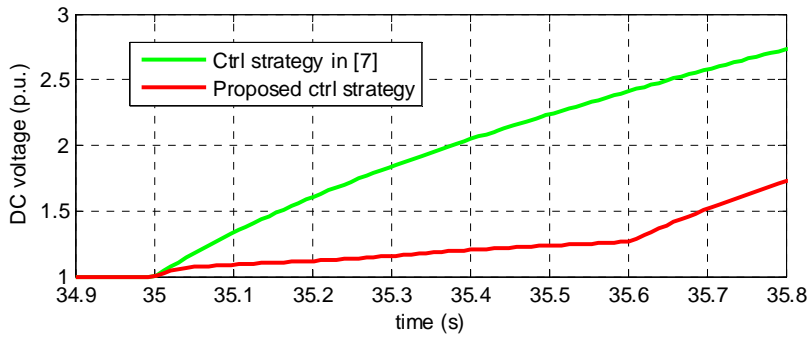


Fig.1.5.38. DC link voltage of the wind turbine in case 2

Case 3 - load event:

The wind power and the PCC voltage in case 3 are presented in Fig. 1.5.39 and Fig. 1.5.40 respectively. During the load event, the PCC voltage decreases below 0.88 p.u. Then the control strategy in [7] reduces the converter output current according to the PCC voltage drop. On the contrary, the proposed control strategy increases the output active current to keep the output power almost constant (as shown in Fig. 1.5.39), and generate a reactive current to support PCC voltage (as shown in Fig. 1.5.40).

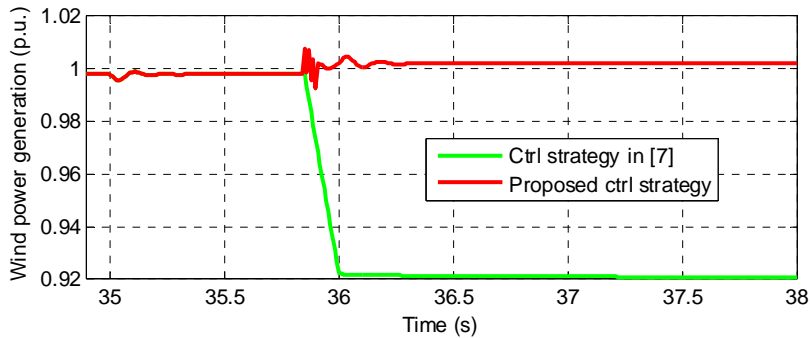


Fig.1.5.39. Wind power generation in case 3

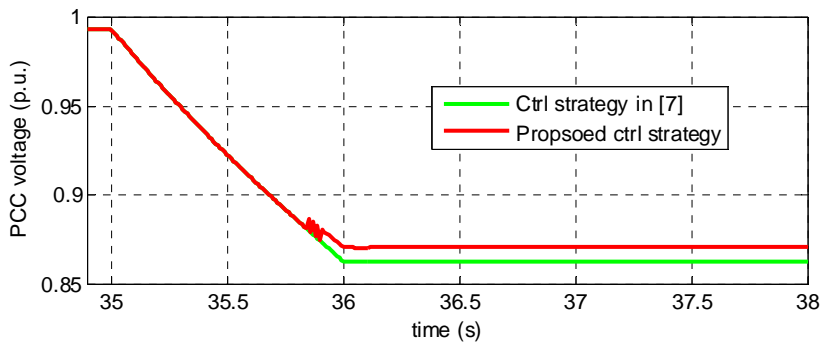


Fig.1.5.40. PCC voltage in case 3

**Conclusions**

DG integration in distribution system can influence the coordination between recloser and fuse in fuse-saving practice. To solve this problem, a new control strategy of the DG converter during fault is proposed by the AAU team.

This strategy uses both PCC voltage and current measurements to decide if it is necessary to reduce the output current under a fault condition. In addition, it can also recognize those non-fault events with voltage drop and provide PCC voltage support. Simulation studies of a test feeder with a full-converter based wind turbine are conducted in DIGSILENG PowerFactory. The results validate the effectiveness of this new control strategy in maintaining recloser-fuse coordination, and its advantage over the previous control strategy in avoiding unnecessary interruption to DG generation during high impedance faults and non-fault events.

This work has been published in a scientific paper titled "An adaptive control strategy of converter based DG to maintain protection coordination in distribution system", and presented in The 5th IEEE PES Innovative Smart Grid Technologies (ISGT) European 2014 Conference, 2014.



## Further research

The previously described control methods can effectively mitigate the influence of DG integration on protection coordination. However, the satisfying performance of this method is limited to a distribution system of simply topology, and with very limited number of DGs integrated. If the topology of the distribution system is complicated so that reconfiguration is inevitable in some scenarios, or if the number of DGs integrated into the distribution system is so large that islanding operation is possible, adaptive protection settings will be necessary. Under this circumstance, the coordination between the selection of protection settings and the selection of DG control modes becomes of great research interest. The AAU team co-worked with researchers from Norwegian University of Science and Technology, and developed a multi-agent system based protection and control scheme which will be briefly described as follows.

The test system used in this study is a modified version of the IEEE 33 bus test system. As shown in Fig. 1.5.41, this test system contains 17 buses, and 3 DGs (including 2 gas turbine generators and 1 wind turbine generator) are integrated in the distribution feeder. The integration level of DG is sufficient to support all loads in the feeder, which means islanding operation of the feeder is possible. In addition, two lines (between bus 5 and bus 15, and between bus 8 and bus 16) equipped with circuit breakers that are open under normal operation, can be used to mesh the feeder for supply reliability under special operation conditions (e.g. islanding operation). Directional overcurrent relays are adopted in the feeder, which are denoted as  $R_{i-j}$ , where  $i$  and  $j$  are respectively the number of the beginning bus and the ending bus of the relay's protection zone as the primary protection.

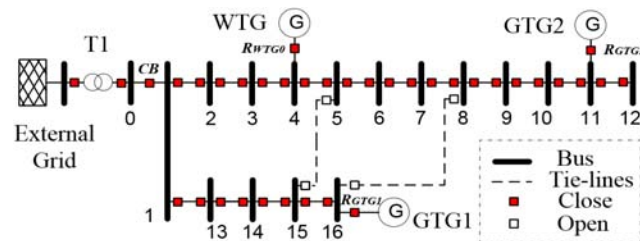


Fig.1.5.41. A test distribution system

Short circuit analysis (during 3 phase fault) is performed in the test feeder to present the impact of DG integration and grid reconfiguration on short circuit currents. The short circuit analysis results at the backward relays comparing the cases without wind turbine, with wind turbine and with wind turbine using special control mode as described in the previous study are given in Fig. 1.5.42. The short circuit analysis results at the forward relays comparing the cases without mesh, with grid-connected mesh and with islanded mesh are given in Fig. 1.5.43. In these two figures, the normal mode is defined as the grid-connected feeder without mesh, connected to a wind turbine without special control. In can be observed in Fig. 1.5.43 that when switching between two configurations, protection system with only one fixed setting may either be oversensitive to large non-fault current (i.e. sympathetic tripping) or face difficulty in sensing the real fault currents in time (i.e. protection blinding). Moreover, when the protection is too slow to sense the fault current, the low-voltage protection of the wind turbine may trip this DG unit unexpectedly. In can be observed in Fig.1.5.42 that the proposed current control method of wind turbine during faults can effectively mitigate the impact of DG integration on short circuit currents. However, since the configuration of the feeder may change in the real practice, the setting for the DG controller to activate this special control should change accordingly. Therefore, on the one hand, DG controller needs the information of the feeder configuration; on the other hand, the protection devices need the information of close DG integration (i.e. DG is connected or not, special control can be activated or not). A smart coordinative protection and DG control strategy is required.

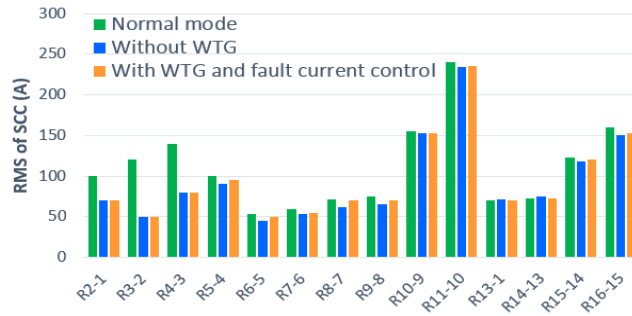


Fig.1.5.42. Short circuit currents for various wind turbine cases

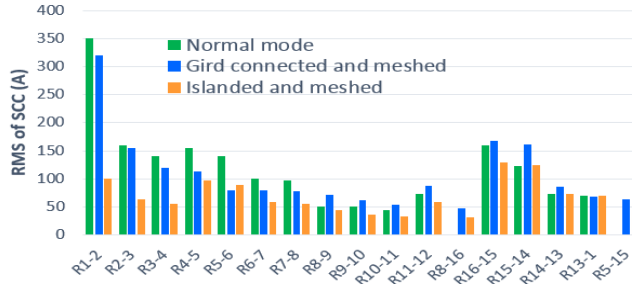


Fig.1.5.43. Short circuit currents for various grid configuration cases

The team proposed a multi-agent based protection and control system (MPCS) to prevent unexpected relay operation due to grid reconfiguration and DG integration. Three control levels are used as shown in Fig.1.5.44, namely, the agent level, the cooperation society level and the control center. The agent level includes DG agent (DGA), and relay agent (RA). The group of agents with necessary information exchange in between is mapped into one cooperation society. A cooperation society is in charge of coordinate information and commands among its group agent. The control center collects grid-wide information, identifies the configuration and operation mode, and accordingly modifies the mapping of agent members into cooperation societies.

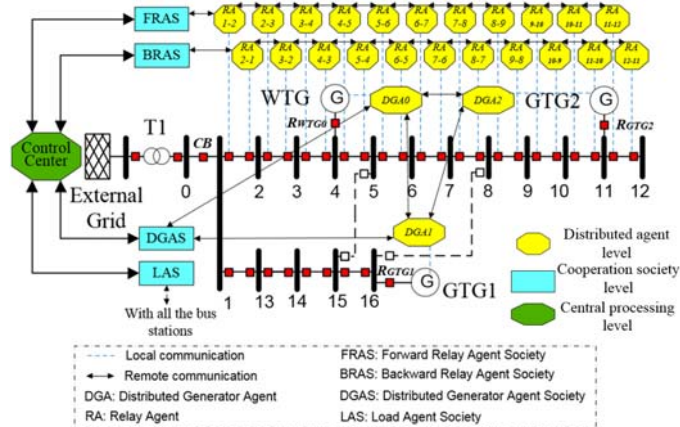


Fig.1.5.44. Structure of MPCS

In the proposed MPCS, DGA adopts the proposed DG control method in the previous study. It collects voltage and current information of the close relays from the cooperation society it belongs, and decides if the special DG control should be activated. It also collects configuration information from the control center to decide what settings should be used as the reference for the voltage and current comparison. RA collects DG connection and control mode information of the related DG from the cooperation society it belongs, and also information about grid configuration from the control center, and decides what protection setting should be implemented.

A hardware-in-the-loop (HIL) platform was built and used to validate the proposed MPCS. As presented in Fig.1.5.45, this platform is based on opal-RT's eMEGAsim simulator and ABB RED670 relays.

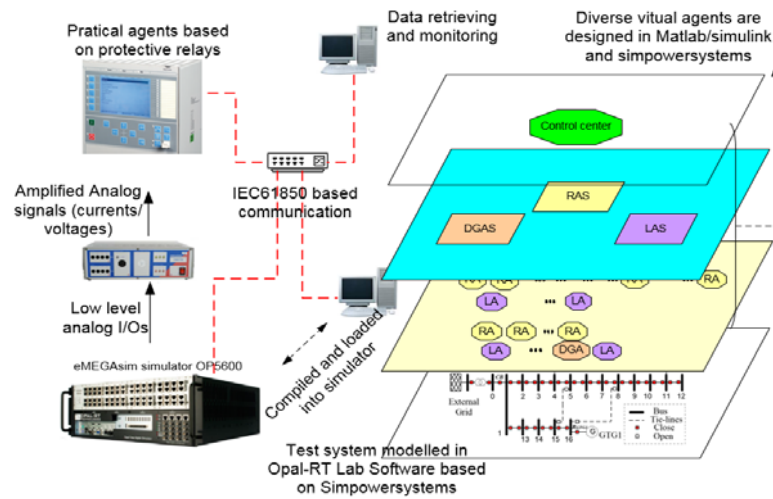


Fig.1.5.45. HIL simulation platform

One scientific paper titled "A Multi-Agent System Based Protection and Control Scheme for Distribution System with Distributed Generation Integration" has been submitted to IEEE Transaction on Power Delivery, and at the present is in the second revision. For this reason, the details of the proposed method and the simulation results are not given here.

#### 1.5.1.2.5 DG control strategies in post-fault stage

After a fault, some parts of a distribution system may be islanded. In this situation, the DGs in the island may have two options: to disconnect and shut down [2][13][14], or to continue operating in an islanded mode [37]. Although islanding operation is expected to increase the reliability of power supply to the customers, there are still various issues to be solved before islanding operation can be practically implemented. In the PRO-NET project, the AAU team mainly focuses on the contribution of PMSG based wind turbines to the frequency control and voltage control of an islanded distribution system. The scopes and limitations of the study by the AAU team in this subject include:

- It is assumed that in the islanded distribution system, there are both directly-connected synchronous generators and power electronic interfaced DGs (e.g. PMSG based wind turbines), so that the grid forming [38] task is performed by directly-connected synchronous generators while power electronic interfaced DGs are controlled to provide frequency and voltage support.
- The PMSG based wind turbines are assumed to work in an MPPT manner in normal conditions. Therefore, when islanding occurs, only down-regulation of power could be provided by the PMSG based wind turbines to support the frequency if the frequency is above the rated value. In other words, no de-load or active power reserve is implemented in the PMSG based wind turbines, so that they don't participate in frequency support when the frequency is below the rated value (which can be supported by other manners, e.g. load shedding or energy storage regulation).
- A communication-based islanding detection method is assumed to be implemented by the distribution system, so that all the DG units in the islanded grid could be aware of the islanding situation in time.
- It is assumed that the imbalance between the generation of the DGs and the consumption of the loads in the distribution system is small at the moment of islanding.

#### Control methods

In the PRONET project, the AAU team proposed control methods for the PMSG based wind turbines to participate in frequency control and voltage control in an islanded distribution system, which will be described in this part.

The frequency controller proposed for the PMSG based wind turbines is shown in Fig. 1.5.46. The input frequency measurement signal  $f$  has a deadband of 0.04Hz, which means a frequency deviation smaller than 0.04Hz from the rated frequency won't be treated by this frequency controller.

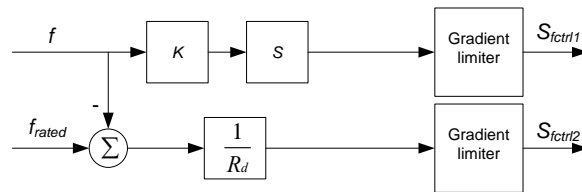


Fig.1.5.46. Proposed frequency controller

Two control loops are used in this controller. The lower control loop is for primary frequency control. The output of this control loop,  $S_{fctrl2}$  is proportional to the deviation of the system frequency from its rated value.  $S_{fctrl2}$  is sent to the pitch angle controller (Fig.1.5.4) and combined into *Pitch*.

The upper control loop is used for inertia emulation. The output of this control loop,  $S_{fctrl1}$ , is proportional to the rate of change of the frequency in the grid. Two options have been considered and compared. The first is to send  $S_{fctrl1}$  also to the pitch controller (as in Fig.1.5.4), and added into *Pitch*. The second is to send  $S_{fctrl1}$  to the grid side convertor controller (as in Fig.1.5.6), and added to the DC voltage reference signal.

Fig. 1.5.47 presents the proposed voltage controller for PMSG based wind turbines.

The voltage at the wind turbine connection point is measured and its difference from the reference voltage value is PI controlled. The output of this controller,  $S_{vctrl}$ , is sent to the grid-side convertor controller as the reactive power reference.

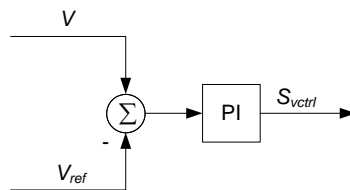


Fig.1.5.47. Proposed voltage controller

### Test system

The IEEE 13-bus system is used as the test system in this study. The original data of the system can be found in [39]. Some modifications have been made on the test system model in order to use it for islanding operation study. These modifications include 5 PMSG based wind turbines (0.5MW each) connected respectively at buses 632, 633, 671, 675 and 692, and a directly-connected synchronous generator (1MW) at bus 680. The modified test system is shown in Fig.1.5.48. The total load in the test system is around 3.5MW.

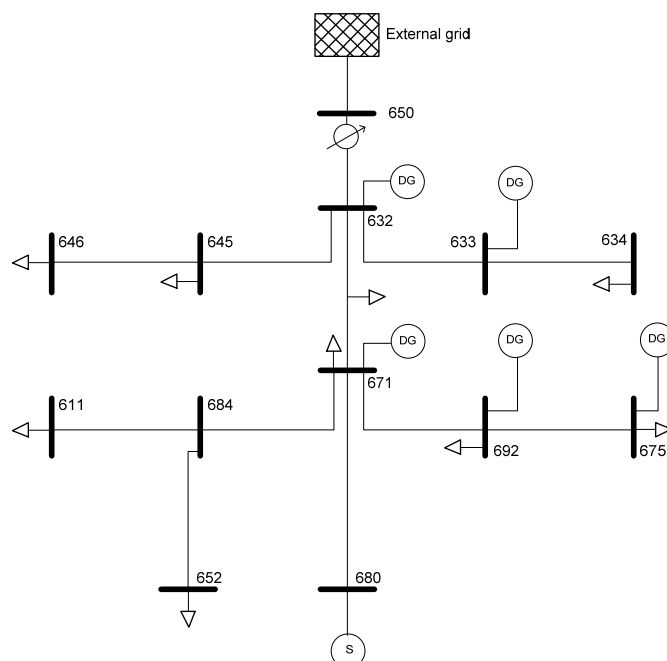


Fig.1.5.48. Modified IEEE 13-bus test system

The test system can be islanded by disconnecting bus 650 from the external grid, and at the same time an islanding detection signal will be sent to those units and controllers in the islanded grid which need to be aware of the islanding condition.

Both the frequency controller and the voltage controller for PMSG based wind turbines are managed by the islanding detection signal, as illustrated in Fig.1.5.49. These two controllers are specially used for the islanding operation, which means if an islanding situation is detected, these two controllers will be switched on, otherwise they are out of service.

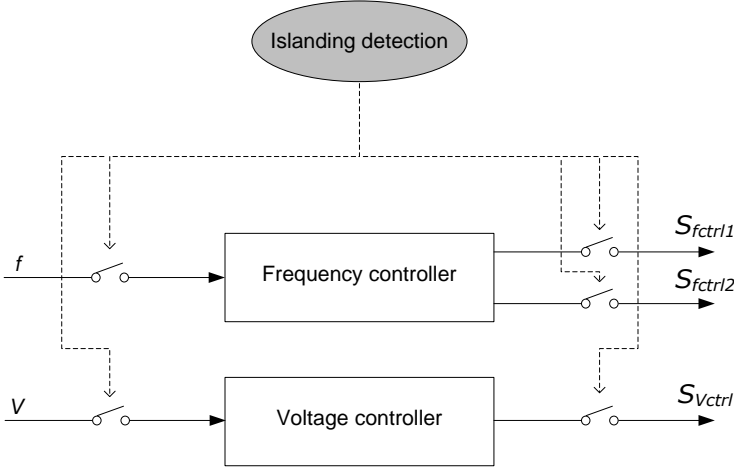
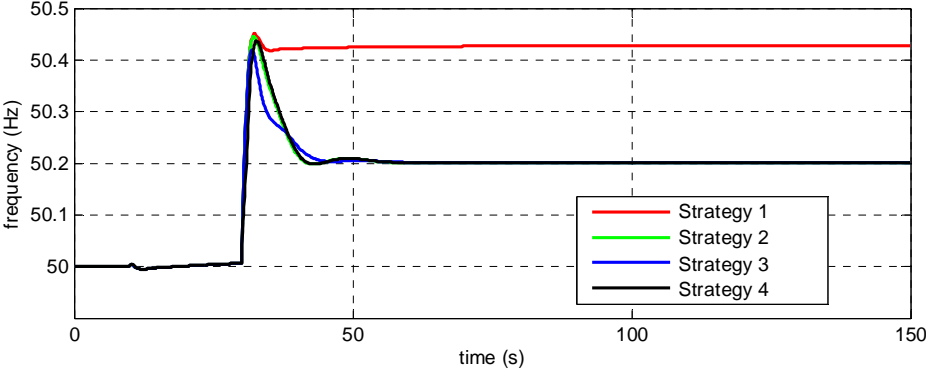


Fig.1.5.49. Controllers managed by islanding detection signal

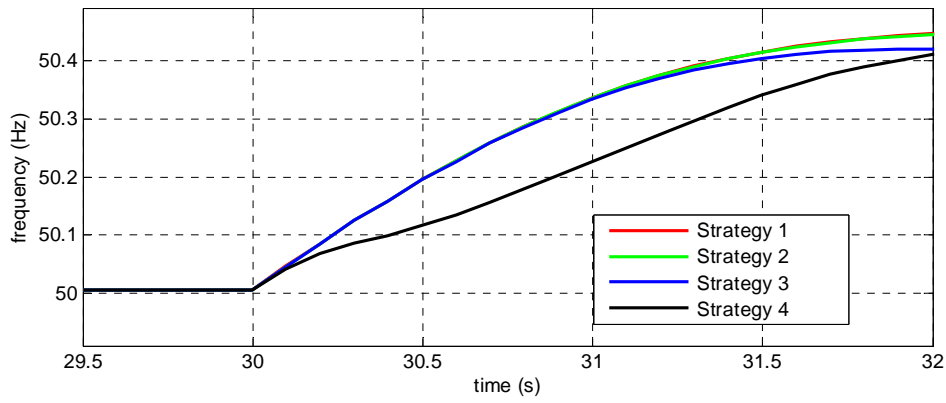
**Simulation results**

Two study cases will be presented here to show the performance of the controllers. In both cases, all the 5 wind turbines are operating with a wind speed of 8m/s, which is below the rated wind speed, and all wind turbines generate 221kW of active power. The test distribution system is islanded at the time 10s, and the frequency controller and voltage controller in the wind turbines are then activated by the islanding detection signal.

In the first study case (case 1), a 140kW load drop event occurs in the islanded grid at the time 30s, immediately followed by frequency rise in the grid. Four options of the wind turbine control strategies are simulated, including the strategy with no frequency control in wind turbines (**strategy 1**), the strategy with only primary frequency control in wind turbines (**strategy 2**), the strategy with both primary frequency control and inertia emulation control implemented in pitch controller (**strategy 3**), and the strategy with both primary frequency control and inertia emulation control implemented in DC voltage controller (**strategy 4**). The results of the frequency in the islanded grid and the electrical power generated by the wind turbine at bus 632 (the other wind turbines have similar performance) are presented in Fig.1.5.50 and Fig.1.5.51 respectively.

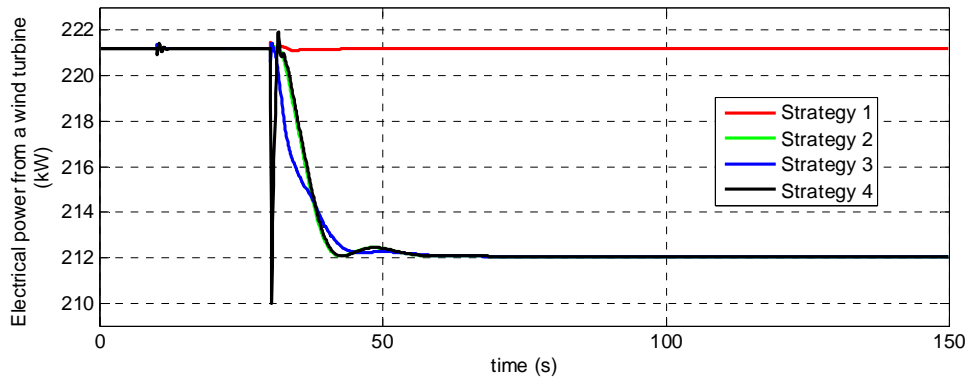


(a)

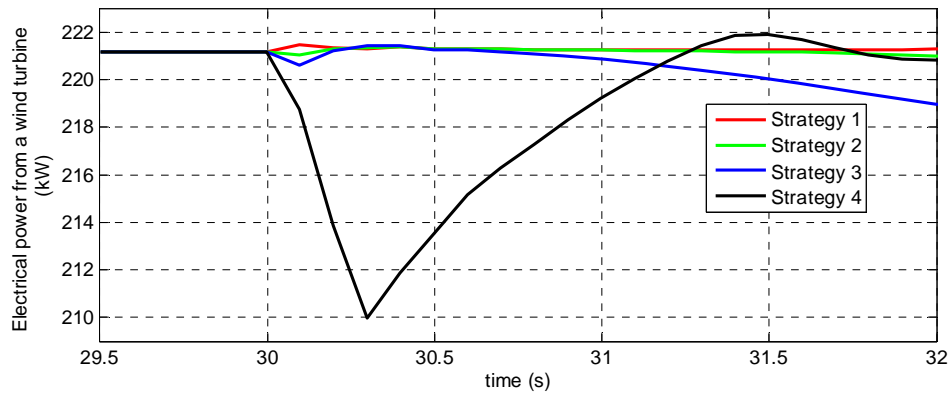


(b)

Fig.1.5.50. Frequency of the islanded distribution system in case 1



(a)



(b)

Fig.1.5.51. Electrical power generated by a wind turbine in case 1

It could be observed in Fig.1.5.50 (a) and Fig.1.5.51 (a) that after the frequency rise event occurs in the islanded distribution system, the output electrical power of the wind turbine will be reduced if the primary frequency control is applied to support the frequency regulation, and the steady state frequency with primary control (i.e. the strategies 2, 3, and 4) is much closer to the rated frequency compared to the red curve with no frequency control (i.e. strategy 1).

Fig.1.5.50 (b) and Fig.1.5.51 (b) are the partial enlarged drawing of Fig.1.5.50 (a) and Fig.1.5.51 (a) respectively, and give more details during the period when the islanded system frequency rises. In Fig.1.5.50 (b), it can be observed that during the frequency-rising period, the red (strategy 1), green (strategy 2) and blue (strategy 3) curves almost rise align with each other, while the black curve (strategy 4) is lower than the others. This means, using strategy 4, the system presents higher inertia than the other three strategies. This could be explained by observations in Fig.1.5.51 (b), in which the black curve (strategy 4) presents a drastic power drop during the frequency-rising period, while the red and green curves (strategies 1 and 2) almost stay flat. The blue curve

(strategy 3) also presents certain power drop, but it is small and too slow compared with the black curve. However, both strategy 3 and strategy 4 are with inertia emulation control implemented, further explanations will be given next about why strategy 4 outperforms strategy 3 in improving the system inertia.

In strategy 3, the inertia emulation is implemented through the pitch angle controller, while in strategy 4, the inertia emulation is implemented through the grid side convertor controller. It is easy to think the difference in the response speed of the pitch angle controller and the DC voltage controller causes the different performance of the two strategies in improving system inertia. However, observing the pitch angle response in strategy 3 during the frequency-rising period as shown in Fig.1.5.52 and the DC voltage response in strategy 4 during the frequency-rising period as shown in Fig.1.5.53, it is difficult to say that the pitch angle response is slower, although the rate of change of the pitch angle is limited in a practical range (2 degree/s in this study).

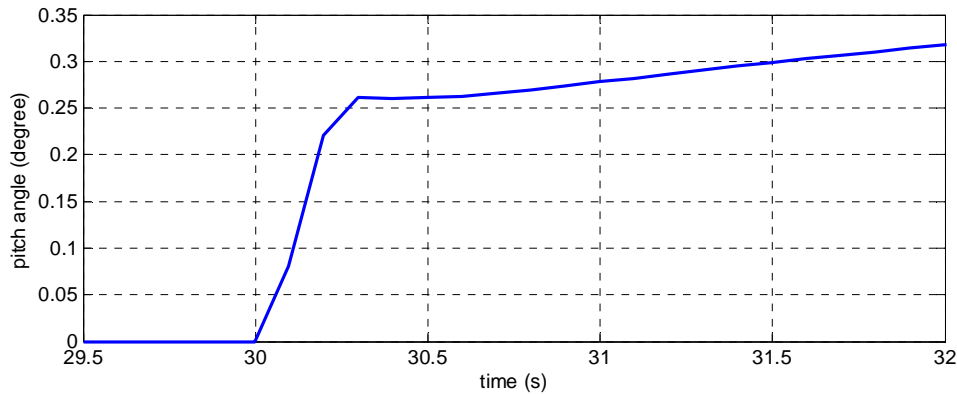


Fig.1.5.52. Pitch angle response in strategy 3 in case 1

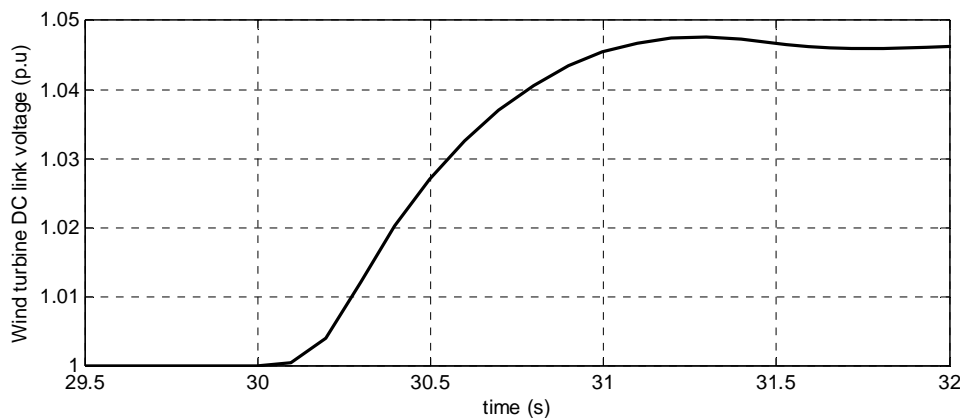


Fig.1.5.53. Wind turbine DC link voltage response in strategy 3 in case 1

Further study has been conducted in strategy 3 to compare the mechanical power absorbed by the wind turbine from the wind with the electrical power generated by the wind turbine to the grid, which is presented in Fig.1.5.54. It can be observed that the mechanical power presents a drastic drop during the frequency-rising period, while the electrical power presents very slow drop. This is the reason why strategy 4 outperforms strategy 3 in inertia emulation, because in strategy 4 the inertia emulation control directly effects on the electrical power to the grid, while in strategy 3, the inertia emulation control effects directly on the mechanical power absorbed from the wind, and the effects will take time to be seen in the electrical power to the grid (due to the response of the intermediate components, e.g. the shaft system, PMSG, generator side convertor) that actually has impact on the system frequency.

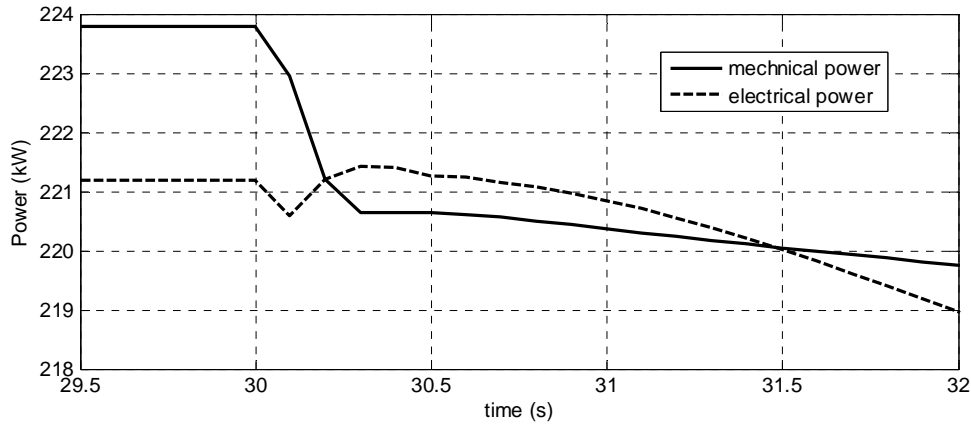


Fig.1.5.54. Mechanical power absorbed by and electrical power generated by a wind turbine in strategy 3 in case 1

In the second study case (case 2), a 400kVAR load rise event occurs in the islanded grid at the time 30s, immediately followed by voltage drop in the grid. The wind turbine control strategies with and without voltage control are simulated, and the results of the voltage and the reactive power generated from the wind turbine at bus 632 (the other wind turbines have similar performance) are presented in Fig.1.5.55 and Fig.1.5.56 respectively.

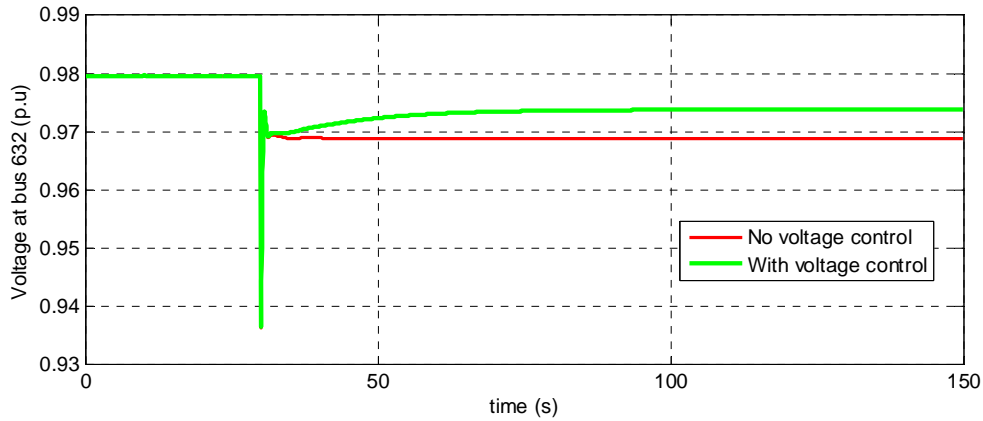


Fig.1.5.55. Voltage at bus 632 in case 2

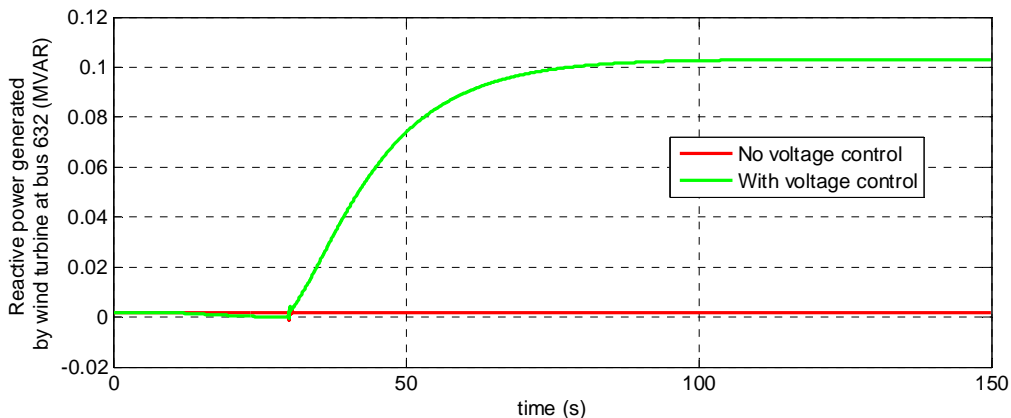


Fig.1.5.56. Reactive power generated by a wind turbine in case 2

It could be observed in Fig.1.5.55 and Fig.1.5.56 that when the voltage drop event occurs in the islanded distribution system, the voltage control can increase the reactive power generated by the wind turbine to support the voltage regulation, so that the steady state voltage in the grid with voltage control is closer to the rated voltage compared to the red curve with no voltage control.

### Conclusion

The AAU team in the PRONET project develops control strategies for PMSG based wind turbine to participate in frequency and voltage control when the connected distribution



system is islanded. The frequency control includes two control loops, i.e. the primary control loop and the inertia emulation control loop. The primary control loop outputs to the pitch controller, and two options of the inertia emulation control loop outputs have been implemented, compared and analyzed. The inertia emulation that outputs to the DC voltage controller is found to really improve the inertia, while the inertia emulation that outputs to the pitch controller doesn't. The reason is that the former can effect directly on the electrical power to the grid, while the latter cannot, and its effect is directly on the mechanical power which will take time to be seen in the electrical power. The voltage control is a PI controller implemented in the grid side convertor controller. Simulation results show the effectiveness of these controllers.

#### 1.5.1.2.6 Reference

- [1] R. Leelaruji and L. Vanfretti, "State-of-the-art in the industrial implementation of protective relay functions, communication mechanism and synchronized phasor capabilities for electric power systems protection," *Renewable and Sustainable Energy Reviews*, vol. 16, pp. 4385-4395, 2012.
- [2] R. C. Dugan and T. E. McDermott, "Distributed generation," *IEEE Industry Applications Magazine*, Mar / Apr. 2002
- [3] T. S. Ustun, C. Oansoy and A. Zayegh, "Recent developments in microgrids and example cases around the world – a review," *Renewable and Sustainable Energy Reviews*, vol. 15, pp. 4030-4041, 2011.
- [4] A. S. Abdel-Khalik, A. A. Elserougi, A. M. Massoud and S. Ahmed, "Fault current contribution of medium voltage inverter and doubly-fed induction-machine-based flywheel energy storage system," *IEEE Trans. Sustain. Energy*, vol. 4, no. 1, pp. 58-67, Jan. 2013.
- [5] N. Nimpitiwan, G. T. Heydt, R. Ayyanar and S. Suryanarayanan, "Fault current contribution from synchronous machine and inverter based distribution generators," *IEEE Trans. Power Del.*, vol. 22, no. 1, pp. 634-641, Jan. 2007.
- [6] A. Darwish, A. S. Abdel-Khalik, A. Elserougi, S. Ahmed and A. Massoud, "Fault current contribution scenarios for grid-connected voltage source inverter-based distributed generation with an LCL filter," *Electric Power Systems Research*, vol. 104, pp. 93-103, 2013.
- [7] H. Yazdanpanahi, Y. Li and W. Xu, "A new control strategy to mitigate the impact of inverter-based DGs on protection system," *IEEE Trans. Smart Grid*, vol. 3, no. 3, pp. 1427-1436, Sep. 2012.
- [8] R. A. Walling, R. Saint, R. C. Dugan, J. Burke and L. A. Kojovic, "Summary of distributed resources impact on power delivery systems," *IEEE Trans. Power Del.*, vol. 23, no. 3, pp. 1636-1644, Jul. 2008.
- [9] E. J. Coster, J.M. A. Myrzik, B. Kruimer and W. L. Kling, "Integration issues of distributed generation in distribution grids," *Proceedings of the IEEE*, vol. 99, no. 1, pp. 28-39, Jan. 2011.
- [10] F. Coffe, C. Booth, A. Dysko and G. Burt, "Quantitative analysis of network protection blinding for systems incorporating distributed generation," *IET Gener., Transm., Distrib.*, vol. 6, iss. 12, pp. 1218-1224, 2012.
- [11] H. Wan, K. K. Li and K. P. Wong, "An adaptive multiagent approach to protection relay coordination with distributed generators in industrial power distribution system," *IEEE Trans. Indust. Applic.*, vol. 46, no. 5, pp. 2118-2124, Sep/Oct. 2010.
- [12] A. Girgis, and S. Brahma, "Effect of distributed generation on protective device coordination in distribution system," *Proc. LESCOPE 01. Large Engineering Systems Conf. Power Engineering*, Halifax, NS, Canada, 2001.
- [13] IEEE Standard for Interconnecting Distributed Resources into Electric Power Systems, IEEE Standard 1547<sup>TM</sup>, Jun. 2003.
- [14] IEEE Application Guide for IEEE Standard for Interconnecting Distributed Resources into Electric Power Systems, IEEE Standard 1547.2<sup>TM</sup>, Apr. 2009.
- [15] P. Mahat, Z. Chen and B. Bak-Jensen, "Review on islanding operation of distribution system with distributed generation," in *Proceedings of the 2011 IEEE Power & Energy Society General Meeting*, Detroit, US, Jul. 2011.
- [16] J. J. Justo, F. Mwasilu, J. Lee and J. Jung, "AC-microgrids versus DC-microgrids with distributed energy resources: a review," *Renewable and Sustainable Energy Reviews*, vol. 24, pp. 387-405, 2013.
- [17] P. Mahat, Z. Chen, B. Bak-Jensen and C. L. Bak, "A simple adaptive overcurrent protection of distribution systems with distributed generation," *IEEE Trans. Smart Grid*, vol. 2, no. 3, pp. 428-437, Sep. 2011.
- [18] A. Dysko, G. M. Burt, S. Galloway, C. Booth and J. R. McDonald, "UK distribution system protection issues," *IET Gener., Transm., Distrib.*, vol. 1, iss. 4, pp. 679-687, 2007.
- [19] P. Kundur, *Power System Stability and Control*. New York: McGraw-Hill, 1994, pp. 699-825.
- [20] S. K. Salman and I. M. Rida, "Investigating the impact of embedded generation on relay settings of utilities' electrical feeders," *IEEE Trans. Power Del.*, vol. 16, no. 2, pp. 246-251, Apr. 2001.
- [21] I. Xyngi, A. Ishchenko, M. Popov and L. van der Sluis, "Transient stability analysis of a distribution network with distributed generators," *IEEE Trans. Power Syst.*, vol. 24, no. 2, pp. 1102-1104, May. 2009.
- [22] H. Lee, G. Son and J. Park, "A study on wind-turbine generator system sizing considering overcurrent relay coordination with SFCL," *IEEE Trans. Appl. Supercond.*, vol. 21, no. 3, pp. 2140-2143, Jun. 2011.
- [23] C. A. Plet and T. C. Green, "Fault response of inverter interfaced distributed generators in grid-connected applications," *Electric Power Systems Research*, vol. 106, pp. 21-28, 2014.
- [24] W. K. A. Najy, H. H. Zeineldin and W. L. Woon, "Optimal protection coordination for microgrids with grid-connected and islanded capability," *IEEE Trans. Indust. Elec.*, vol. 60, no. 4, pp. 1668-1677, Apr. 2013.
- [25] M. Baran and I. El-Markabi, "Adaptive over current protection for distribution feeders with distributed generators," *Proc. IEEE Power Eng. Soc.*, vol.2, pp. 715-719, Oct. 2004.
- [26] J. Ma, X. Wang, Y. Zhang, Q. Yang and A. G. Phadke, "A novel adaptive current protection scheme for distribution systems with distributed generation," *Electrical Power and Energy Systems*, vol. 43, pp. 1460-1466, 2012.
- [27] E. Sortomme, S. S. Venkata and J. Mitra, "Microgrid protection using communication-assisted digital relays," *IEEE Trans. Power Del.*, vol. 25, no. 4, pp. 2789-2796, Oct. 2010.
- [28] I. Chilvers, N. Jenkins and P. Crossley, "Distance relaying of 11kV circuits to increase the installed capacity of distributed generation," *IEE Proc. Gener. Transm. Distrib.*, vol.152, no. 1, pp. 40-46, Jan. 2005.
- [29] N. Rezaei and M. -R. Haghifam, "Protection scheme for a distribution system with distributed generation using neural networks," *Electrical Power and Energy Systems*, vol. 30, pp. 235-241, 2008.
- [30] S. A. M. Javadian, M. -R. Haghifam, S. M. T. Bathaee and M. Fotuhi Firoozabad, "Adaptive centralized protection scheme for distribution systems with DG using risk analysis for protective devices placement," *Electrical Power and Energy Systems*, vol. 44, pp. 337-345, 2013.
- [31] H. Zayandehroodi, A. Mohamed, M. Farhoodnea and M. Mohammadjafari, "An optimal radial basis function neural network for fault location in a distribution network with high penetration of DG units," *Measurement*, vol. 46, pp. 3319-3327, 2013.

- [32] H. Zayandehroodi, A. Mohamed, H. Shareef and M. Farhoodnea, "A novel neural network and backtracking based protection coordination scheme for distribution system with distributed generation," *Electrical Power and Energy Systems*, vol. 43, pp. 868-879, 2012.
- [33] G.D. Moor, and H.J. Beukes, "Maximum power point trackers for wind turbines," in *Proc. of 35th Annual IEEE Power Electronics Specialists Conference*, Aachen, Germany, Jun. 2004, pp. 2044–2049.
- [34] T. Senjyu, T. Shimabukuro, , and K. Uezato, "Vector control of permanent magnet synchronous motors without position and speed sensors," in *Proc. of 26th Annual IEEE Power Electronics Specialists Conference*, Atlanta, USA, Jun. 1995, pp. 759–765.
- [35] S. Hadi, *Power System Analysis*, McGraw Hill Inc., 2010, pp: 399-459.
- [36] F. Coffele, C. Booth, A. Dysko and G. Burt, "Quantitative analysis of network protection blinding for systems incorporating distributed generation," *IET Gener., Transm., Distrib.*, vol. 6, iss. 12, pp. 1218-1224, 2012.
- [37] P. Mahat, "Control and operation of islanded distribution system", PhD thesis, Aalborg University, Denmark, 2010.
- [38] J. Rocabert, A. Luna, F. Blaabjerg and P. Rodriguez, "Control of power convertors in AC microgrids," *IEEE Trans. Power Electron.*, vol. 27, no. 11, pp. 4734-4749, Nov. 2012.
- [39] <http://ewh.ieee.org/soc/pes/dsacom/testfeeders/>

### **1.5.1.3 Tasks conducted by other partners**

All three partners in the consortium have made important contributions to the technical results in the PRO-NET project. This section (1.5.1.3) will briefly introduce the main research activities and technical results by the Turkish team (TUBITAK UZAY) and the Norwegian team (SIMULA).

#### **Research activities and technical results by TUBITAK UZAY**

The Turkish team has analysed the uncertainty of DG systems such as wind and solar energy conversion systems. In addition, the integration of DG units to grid leading to new local energy sources has been studied. Two main types of control schemes of power electronics based DG have been considered, namely current control scheme and voltage control scheme. Static modelling of the two control schemes for load flow and fault analysis has been performed and the results have been submitted to an IEEE journal, which is now under review. Such characteristics investigation shows that mis-operations and imperfect selectivity of relays can occur within the distribution system. These issues call for the need of a bi-directional relay operation.

The Turkish team then proposed a new adaptive protection scheme for distribution systems with DG. The contribution of the study is to combine the impacts of availability scenarios for multiple DG units with protection schemes in a dynamic structure, which is ignored in previous studies that consider static structures without possible operating modes related to DG unit's availability issue. Results on an IEEE 4-node distribution system show that the proposed algorithm can perform adaptive relay coordination under various fault conditions. Compared with the conventional protection structure, relay coordination of adaptive protection scheme provides fast fault isolation and greater adaptation to different operating modes considering DG units.

The Turkish team also proposed an adaptive protection strategy for a distribution system with DG integration considering both grid-connected and islanded operation modes of the distribution system. The proposed strategy considers both grid-connected and islanded operating modes while the adaptive operation of the protection is dynamically realized considering the availability of DG power production (related to faults or meteorological conditions) in each time step. Besides, the modular structure and fast response of the proposed strategy is validated via simulations conducted on the IEEE 13-Node Test System.

#### **Research activities and technical results by SIMULA**

The Norwegian team achieved the objective "determine cost effective and reliable communication system to support the protection and control methods" with three strategies: new Machine-to-Machine (M2M) communications, intelligent demand response management, and secure schemes for efficient and reliable smart grid.

For the advanced communications solution, mainly two key challenges, i.e. quality of service (QoS) and energy-efficiency, have been addressed. A new time-division spectrum sensing strategy has been presented. The main advantage of this solution is the largely reduced control messages overhead with a decentralized architecture. For the demand response management, a dependable and reliable smart grid has been proposed. New game-theory based model has been proposed to achieve global optimization and end-to-end reliability. For secure schemes, context-aware authentication schemes have been proposed to defend cyber-attacks and protect battery-status private information. This is able to protect critical Vehicle-to-Grid systems as well as the power grid infrastructure.

### **1.5.2 Reflections on the problems stated in the application**

The PRONET project has fulfilled its objectives. The new characteristics of the distribution system with large number of renewable energy generation units and power electronic interfaced devices have both been studied in the literature and investigated through simulation work based on the models that have been developed in the project for the representation of the distribution system, the power electronics-interfaced renewable generation units, and the protection system. Communication based adaptive methods have been developed for the purpose of mitigating the negative impacts of electronics-interfaced renewable generation integration on the performance of protection in distribution systems, including solutions from the protection perspective, or DG control perspective, or the perspective of coordination between protection and DG control. Control strategies for DGs to support the stability and power quality of a post-fault islanded distribution system have also been developed. Cost effective and reliable communication system to support the protection and control methods in distribution system has been achieved through three strategies, i.e. new Machine-to-Machine (M2M) communications, intelligent demand response management, and secure schemes for efficient and reliable smart grid. Hardware-in-the-loop platforms have been built to evaluate the performance of the whole system.

All these investigations and solutions focus on the targets to make the distribution system adaptive to more renewable energy integration, and be able to operate with higher reliability (including feasibility of islanding operation), which could increase the utilization of renewable energy in power systems both in scale and in time. EU countries have agreed on some ambitious climate and energy framework (e.g. 2030 Framework for climate and energy), while renewable energy penetration in power systems is one of the main measures in Europe in order to meet those environmental targets. Therefore, the PRONET project has lived up to the expectations in terms of contributions to the European environmental sustainability.

### **1.5.3 Dissemination**

Scientific publications in journals and conferences are the major dissemination activities. Research papers that have been submitted by the AAU team to scientific journals and conferences for publications include:

- [1] Z. Liu, C. Su, H. K. Høidalen and Z. Chen, "A Multi-Agent System Based Protection and Control Scheme for Distribution System with Distributed Generation Integration", submitted to *IEEE Transactions on Power Delivery*, accepted.
- [2] Z. Liu, Z. Chen, H. Sun and Y. Hu, "Multiagent System-Based Wide-Area Protection and Control Scheme against Cascading Events", *IEEE Trans. Power Del.*, vol. 30, no. 4, pp. 1651-1662, Aug. 2015.
- [3] C. Su, Z. Liu, Z. Chen and Y. Hu, "An adaptive control strategy of converter based DG to maintain protection coordination in distribution system," in Proc. IEEE PES Innovative Smart Grid Technologies, Europe (ISGT 2014 Europe), Istanbul, Turkey, Oct 2014.
- [4] C. Su, Z. Liu, Z. Chen and Y. Hu, "Short circuit analysis of distribution system with integration of DG," in Proc. International Conference on Power System Technology (POWERCON 2014), Chengdu, China, Oct 2014.
- [5] Z. Liu, Z. Chen and Y. Hu, "Detection of Vulnerable Relays and Sensitive Controllers under Cascading Events Based on Performance Indices," in Proc. IEEE PES General Meeting 2014, Washington, US, 2014.
- [6] M. Wei, Z. Chen, "Fast Control Strategy for Stabilizing Fixed-speed Induction Generator Based Wind Turbines in An Islanded Distributed System", *IET Renewable Power Generation*, vol. 7, no. 2, March 2013, pp. 144-162.

The conference papers [3][4][5] have been successfully presented in ISGT 2014 Europe, POWERCON 2014 and IEEE PES General Meeting respectively.

### **1.6 Utilization of project results**

The technical results of the PRONET project are expected to be utilized by distribution system operators (DSOs), DG unit and protection device manufacturers, and communication system (for distribution system) designers, to build a more reliable, sustainable and economical smart distribution networks, particularly for higher penetration of renewable energy generations. The investigation results of the new characteristics of the distribution systems with large scale of power-electronics-interfaced DGs could be used

as a reference for the development and updating of grid codes by DSOs. The solutions developed in the PRONET project for adaptive protection methods, and DG control strategies during and after faults, can be used by manufacturers and DG owners to match their product and operation manners with the grid requirements without increasing unnecessary cost.

The technical results are also expected to be used as the foundation of further research activities in collaborations with institutions, and industrial and commercial entities in a European or Global level.

Finally, the knowledge obtained in the PRONET project will be utilized in teaching activities related to the topics of distribution system protection, distribution generation control and communication technology in power systems.

### **1.7 Project conclusion and perspective**

The PRONET project has investigated the new characteristics of the distribution system with large number of renewable energy generation units and power electronic interfaced devices. The impacts of DG integration on the short circuit current profiles and the protection performance under both symmetrical and unsymmetrical faults have been studied. It is found that the connection type of the DG transformers plays an important role in these impacts. Various solutions have then been developed in the PRONET project to mitigate the negative impacts of DG integration on protection performance. Regarding the DG control during fault, an adaptive control method have been developed to reduce the short circuit current injected by DGs in selected situations, in order to maintain the coordination among the protection devices. Regarding the protection settings, communication-based adaptive setting methods have been developed considering availability scenarios of multiple DG units, and changing operating conditions (i.e. grid-connected operation and islanding operation). For more complicated distribution network topologies and operation conditions, a multi-agent system based protection and control scheme, coordinating the DG control during fault and the adaptive setting, have been developed and tested in a hardware-in-the-loop platform. Furthermore, control methods for power-electronics-interfaced DG to participate in frequency and voltage control in a post-fault islanded distribution system have been developed.

The technical results of the PRONET project are expected to contribute to more reliable, sustainable and economical distribution systems with increased renewable integration, and to be beneficial for distribution system operators and consumers. These results are in line with EU climate and energy frameworks, and will contribute to the European environmental sustainability.

From the future perspectives, the results and limitations of the PRONET project can be used respectively as the foundation and focused problems for further research activities relevant to the topics of distribution system protection, distribution generation control and communication technology in power systems.

### **Annex**

Relevant publication links:

[2][http://vbn.aau.dk/en/publications/multiagent-systembased-widearea-protection-and-control-scheme-against-cascading-events\(13b5618f-3369-427e-8702-de8ad4c48d4b\).html](http://vbn.aau.dk/en/publications/multiagent-systembased-widearea-protection-and-control-scheme-against-cascading-events(13b5618f-3369-427e-8702-de8ad4c48d4b).html)

[3][http://vbn.aau.dk/en/publications/an-adaptive-control-strategy-of-converter-based-dg-to-maintain-protection-coordination-in-distribution-system\(aca3bd3a-b5f6-4b18-8205-77298ee60fd0\).html](http://vbn.aau.dk/en/publications/an-adaptive-control-strategy-of-converter-based-dg-to-maintain-protection-coordination-in-distribution-system(aca3bd3a-b5f6-4b18-8205-77298ee60fd0).html)

[4][http://vbn.aau.dk/en/publications/short-circuit-analysis-of-distribution-system-with-integration-of-dg\(ff2a018d-d956-4257-9b67-c79daec04ef2\).html](http://vbn.aau.dk/en/publications/short-circuit-analysis-of-distribution-system-with-integration-of-dg(ff2a018d-d956-4257-9b67-c79daec04ef2).html)

[5][http://vbn.aau.dk/en/publications/detection-of-vulnerable-relays-and-sensitive-controllers-under-cascading-events-based-on-performance-indices\(dcf58d1-9129-4989-8fdd-aa4328056495\).html](http://vbn.aau.dk/en/publications/detection-of-vulnerable-relays-and-sensitive-controllers-under-cascading-events-based-on-performance-indices(dcf58d1-9129-4989-8fdd-aa4328056495).html)

[6][http://vbn.aau.dk/en/publications/fast-control-strategy-for-stabilising-fixedspeed-inductiongeneratorbased-wind-turbines-in-an-islanded-distributed-system\(92fc3656-8e0d-42eb-be51-da1b5f420715\).html](http://vbn.aau.dk/en/publications/fast-control-strategy-for-stabilising-fixedspeed-inductiongeneratorbased-wind-turbines-in-an-islanded-distributed-system(92fc3656-8e0d-42eb-be51-da1b5f420715).html)